Ab-initio investigation of metal-insulator transitions in strongly correlated low-dimensional systems

Inaugural-Dissertation
to obtain the academic degree
Doctor rerum naturalium (Dr. rer. nat.)
submitted to the Department of Biology, Chemistry and Pharmacy
of the Freie Universität Berlin

by

Edoardo Fertitta
from Palermo, Italy

Berlin, 2016

This work was prepared under the supervision
of Prof. Dr. Beate Paulus (Freie Universität Berlin)
between May 2013 and May 2016

1. Reviewer: Prof. Dr. Beate Paulus

2. Reviewer: Prof. Dr. Jens Eisert

Date of the defense: July 19^{th} 2016

Ai miei genitori

Acknowledgements

A doctoral dissertation is a stage in one's life that can rarely be considered as the fruit of the work of a single person. Many different people have helped me to reach this result and I would like to thank all them for their wise and foreseeing supervision, precious suggestions, enligthening insights and direct scientific contribution.

First and foremost I would like to express my utmost gratefulness for my supervisor, Prof. Dr. Beate Paulus. During my studies she has been a wise guidance, she gave me the freedom to conduct my research in the way I found more compelling while directing me towards the most promising areas and has strongly contributed to my scientific persona. The key to a fruitful scientific career is undoubtely governed by a unique amalgam of collaboration and communication skills. This is why I would also like to thank her for giving me the chance to attend many scientific conferences, meetings, workshops and to actively collaborate with other workgroups, allowing me to widen my horizons.

I would also like to express my gratitude to Prof. Dr. Jens Eisert for kindly accepting the task of being the second referee for my doctoral dissertation and for showing much interest into my project.

The experiences made abroad have certainly been fundamental to the realization of this work. I thank both our collaborators in Touluse and Budapest for this. This project brought together the research of our workgroup with that of Prof. Dr. Stevano Evangelisti and Prof. Dr. Thierry Leininger of the IRSAMC at the Université de Toulouse. I gratefully acknowledge them for introducing me to their scientific field and for their supervision during my stay in Toulouse. Moreover, I would like to thank Dr. Muammar El Khatib, not only for his valuable scientific support, but also for his friendship. The collaboration with the group of Prof. Dr. Örs Legeza of the Wigner center in Budapest has also been particularly successful and it is my sincere hope that it will bring our common research into many other interesting and compelling areas in the future. I want to thank him and all the members of his group, especially Dr. Gergely Barcza for his precious help, his hard work and constant support.

I would like to thank all members of the AG Paulus, starting from Priv-Dozent Dr. Dirk Andrae. Although not directly involved into my project he has always been open to discussion, rendering many useful and enligthening suggestions, which helped me to work in a more rigorous and meticulous manner. I would also like to mention Daniel Koch and Christian Stemmle for their hard work and collaboration. Being a part of the workgroup of Prof. Paulus has not only been intellectually stimulat-

ing, but has also been an enjoyable experience because of the pleasant and friendly atmosphere. This is of course accredited to all the members of the AG Paulus, AG Keller and AG Trembley and I am glad that among them I found so many good friends: Matthias Berg, Luca Donati, Stevan Aleksić, Francesca Vitalini, Lukas Marsoner, Federica Maschietto and Dr. Jhon Frédy Perez Torres.
This research could not have been possible without the financial support of the German Research Foundation (DFG) and the Agence Nationale de la Recherche (ANR) via the project "Quantum-chemical investigation of the metal-insulator transition in realistic low-dimensional systems" (action ANR-11-INTB-1009 MITLOW PA1360/6-1). The support of the Zentraleinrichtung für Datenverarbeitung (ZEDAT) at the Freie Universität Berlin is gratefully acknowledged. Also I would like to thank the support of the Max Planck Society via the International Max Planck Research School.
Looking back into the path that led me to this stage of my life I feel the need of thanking someone else for deeply shaping my *forma mentis*, passing down to me his love for science and giving me the courage to make the first step to move abroad. Late Prof. Dr. Roberto Triolo has been a mentor for me and many other young sicilian chemists. My only sorrow is that I will not be able to express my gratitude to him in person.
Friends and family, of course, cannot be forgotten. I would like to thank all the people who made my time in Berlin so enjoyable and memorable, especially Laura and Enrico, Michele, Emma, Enrico and Francesca, Selene, Leonardo and Samantha, Florien, Namrata and particularly Menemsha for her dedicated proof reading of this thesis. Special thanks goes to Marco, whom I consider my closest friend and who has been a loyal companion in the last seven years. Also I want to thank my lifelong friends who, even if distant, have always been and always will be an important part of my life: Simone, Daniele, Gabriele and Massimiliano.
Last but not the least, it is hard to express in words my gratitude towards my parents. Their support, guidance and understanding gave me the chance to pursuit my goals in life. The best way to thank them and repay their unconditional love and trust is to keep doing my best in all I do.

Summary

The clear distinction between metals and insulators is a well established and appartently simple concept which can be clarified by studying the behavior of the electrical conductivity. However, a theoretical description of the processes leading to one of the two extremes is no trivial task. The widely accepted band structure theory relies on an one-electron picture to characterize the metallic/insulating behavior of a material. However, in spite of the fact that it can be used to make successful predictions, this description does not capture one of the essential elements characterizing the nature of an electronic quantum system, *i.e.* the electron correlation. The key to the different behaviors is clearly contained in the correlated many-electron wave function, but the analysis of such a high-dimensional object in configuration space can be quite cumbersome. Therefore the development of powerful tools to simplify this task is necessary.

The total position-spread (TPS) tensor, which was derived by Walter Kohn's theory of the insulating state, plays a key role in the field of metal-insulator transitions (MITs). This tool provides information about the electron localization, which is strongly connected to the electrical conductivity. Therefore, in this work particular attention was paid to the calculation of the TPS tensor of small and extended systems. Moreover, part of this thesis focuses on a new formalism, which allows the study of spin mobility and spin entanglement and provides therefore deeper insight into the effects of electron correlation.

In the framework of quantum information theory (QIT), the quantum entanglement can be quantified by means of measures such as the von Neumann entropy. Also, the analysis of the elements of the two-orbital reduced density matrix provides an overview of the complexity of the many-electron wave function. These insights were used in this work for the analysis of the metallic/insulating character of a system.

However, in order to perform such investigastions, the problem of achieving an accurate description of the many-electron wave function has to be dealt with. Despite the tremedous progress in the efficiency of quantum-chemical methods, the treatement of extended systems using standard approaches is still a difficult (if not unfeasible) task. Therefore the development and testing of sophisticated, low-scaling methods is currently the subject of many investigations. In this work, two approaches were employed: 1) the *ab-initio* density matrix renormalization group (DMRG) approach which, based on a tensor

product ansatz, provides very precise results and exploits QIT to improve its performance; 2) the method of increments (MoI) which, using a many-body expansion in terms of localized orbitals, yields accurate correlation energies. By using both methods on strongly correlated one-dimesional model systems, we worked on a new formalism of the method of increments which can be used to describe the whole dissociation curve without inconvenient discontinuities. Finally, aiming to calculate the total position-spread tensor of extended systems, we worked on the application of the MoI for quantities other than the correlation energy.

Zusammenfassung

Der deutliche Unterschied zwischen Metallen und Isolatoren ist ein bekanntes und augenscheinlich einfaches Konzept, das mit dem Verhalten der elektrischen Leitfähigkeit erklärt werden kann. Die theoretische Beschreibung von Prozessen, die zu einem der zwei Extrema führen, ist jedoch nicht trivial. Die weithin akzeptierten Bandstrukturtheorie basiert auf einem Einelektronenbild, um den metallischen/insulierenden Charakter des Materials zu beschreiben. Obwohl es zu vielen erfolgreichen Vorhersagen führt, beschreibt dieses Model gerade eine der essentiellen Elemente eines elektronisches Quantensystems nicht, die sogenannte Elektronenkorrelation. Der Schlüssel zur korrekten Beschreibung der verschiedenen Leitfähigkeiten liegt zweifellos in der korrelierten Mehrelektronenwellenfunktion. Da die Hochdimensionalität eines solchen Objektes im Konfigurationsraum dessen Analyse erschwert, wird die Entwicklung von neuen wirksamen Methoden für solche Aufgaben notwendig.

Ein Analysewerkzeug spielt eine Hauptrolle im Rahmen von Metall-Isolator-Übergängen, der Gesamtortsausbreitungstensor (TPS aus dem Englischen *total position-spread*), der aus Walter Kohns Theorie des Isolatorzustands abgeleitet wurde. Der TPS Tensor enthält Informationen über die Elektronlokalisierung, die stark mit der elektrischen Leitfähigkeit verbunden ist. Deswegen haben wir unser Interesse auf die Berechnung des TPS Tensors für kleine sowie ausgedehnte Systeme ausgerichtet. Außerdem behandelt ein Teil dieser Arbeit einen neuen Formalismus, der die Untersuchung der Spinbeweglichkeit und der Spinverschränkung erlaubt, um ein besseres Verständnis von den Effekten der Elektronkorrelation zu erlauben.

Im Rahmen der Quanteninformationstheorie (QIT), kann die Quantenverschränkung durch Werkzeuge wie die von Neumann Entropie quantifiziert werden. Außerdem erhaltet die Analyse der Elementen von der Zweiorbital reduzierten Dichtematrix Einsicht über die Komplexität der Mehrelektronenwellenfunktion. Solche Untesuchungen wurden in dieser Arbeit für die Analyse der metallischen/insulierenden Charakter eines System genuzt.

Allerdings bedürfen solche Untersuchungen eine genaue Beschreibung der Mehrelektronenwellenfunktion. Trotz der gewaltige Forschritte, die immer genauere quantenchemische Methoden hervorgebracht haben, ist die Behandlung ausgedehnter Systeme mit hohem Aufwand verbunden oder nicht pratikabel. Deshalb ist die Entwicklung und das Testen von neuen hochentwickelten niedrig skalierenden Metho-

den ein sehr aktuelles Thema. In dieser Arbeit wurden zwei von solchen Methoden genutzt: 1) die Dichtematrix Renomierungsgruppe (DMRG), die auf einem Tensorproduktansatz basiert und sehr genaue Ergebnisse erzielt und QIT nutzt; 2) die Inkrementenmethode (MoI aus dem Englischen *method of increments*), die durch eine Vielkörper-Entwicklung in Form von lokalisierten Orbitalen, akkurate Korrelationenergierechnungen erlaubt. Beide Methoden wurden auf stark-korrelierte eindimensionale Systeme angewandet. Dabei haben wir einen neuen Formalismus der Inkrementenmethode entwickelt, der gesamte Dissoziationkurven ohne Unterbrechungen beschreiben kann. Um die Berechnung des TPS Tensors für ausgedehnte Systeme zu ermöglichen, wurde die MoI für diese Große ebenfalls angewendet.

Contents

List of Publications

Paper m1 M. El Khatib, O. Brea, E. Fertitta, G. L. Bendazzoli, S. Evangelisti, T. Leininger
"The total position-spread tensor: spin partition"
J. Chem. Phys. **142**, 094113 (2015)
DOI 10.1063/1.4913734

Paper m2 M. El Khatib, O. Brea, E. Fertitta, G. L. Bendazzoli, S. Evangelisti, T. Leininger, B. Paulus
"Spin delocalization in hydrogen chains described with the spin-partitioned total position-spread tensor"
Theor. Chem. Acc. **134**, 29 (2015)
DOI 10.1007/s00214-015-1625-7

Paper M1 E. Fertitta, M. El Khatib, G. L. Bendazzoli, S. Evangelisti, T. Leininger, B. Paulus
"The spin-partitioned total position-spread tensor: An application to Heisenberg spin chains"
J. Chem. Phys. **143**, 244308 (2015)
DOI 10.1063/1.4936585

Paper M2 E. Fertitta, B. Paulus, G. Barcza, Ö. Legeza
"Investigation of metal-insulator-like transition through the *ab-initio* density matrix renormalization group approach"
Phys. Rev. B **90**, 245129 (2014)
DOI 10.1103/PhysRevB.90.245129

Paper M3 E. Fertitta, B. Paulus, G. Barcza, Ö. Legeza
"On the calculation of complete dissociation curves of closed-shell pseudo-one-dimensional systems via the complete active space method of increments"
J. Chem. Phys. **143**, 114108 (2015)
DOI 10.1063/1.4930861

Paper M4 D. Koch, E. Fertitta, B. Paulus
"Calculation of the static and dynamical correlation energy of pseudo-one-dimensional beryllium systems via a many-body expansion"
J. Chem. Phys. **145**, 024104 (2016)
DOI 10.1063/1.4955317

Paper M5 E. Fertitta, D. Koch, B. Paulus, G. Barcza, Ö. Legeza
"Towards a fully size-consistent method of increments"
arXiv:1605.03904 [physics.chem-ph]
Submitted to *J. Comp. Theor. Chem.* in May 2016

Additional publications

Paper a1 E. Fertitta, E. N. Voloshina, B. Paulus
"Adsorption of multivalent alkylthiols on Au(111) surface: Insights from DFT"
J. Comp. Chem. **35**, 204 (2014)
DOI 10.1002/jcc.23484

Paper a2 E. N. Voloshina, E. Fertitta, A. Garhofer, F. Mittendorfer, M. Fonin, A. Thissen, Yu. S. Dedkov
"Electronic structure and imaging contrast of graphene moiré on metals"
Nature Sci. Rep. **3**, 1072 (2013)
DOI 10.1038/srep01072

Paper a3 S. Haas, R. Fenger, E. Fertitta, K. Rademann
"Cascade catalysis of highly active bimetallic Au/Pd nanoclusters: structure-function relationship investigation using anomalous small-angle X-ray scattering and UV-Vis spectroscopy"
J. Appl. Cryst **46**, 1353 (2013)
DOI 10.1107/S0021889813018190

Paper a4 R. L. Fenger, E. Fertitta, H. Kirmse, A. F. Thunemann, K. Rademann
"Size-Dependent Catalysis with CTAB-Stabilized Gold Nanoparticles"
Phys. Chem. Chem. Phys. **14**, 9343 (2012)
DOI 10.1039/C2CP40792B

List of Figures

List of Abbreviations

ACPF	Averaged coupled pair functional
BCH	Baker-Campbell-Hausdorff
BOA	Born-Oppenheimer approximation
CAS	Complete active space
CC	Coupled cluster
CCS	Coupled cluster singles
CCSD	Coupled cluster singles and doubles
CCSDT	Coupled cluster singles, doubles and triples
CCSDTQ	Coupled cluster singles, doubles, triples and quadruples
CCSD(T)	Coupled cluster singles and doubles with perturbative triples
CI	Configuration interaction
CISD	Configuration interaction singles and doubles
CSCO	Complete set of commuting operators
CSF	Configuration state function
DBSS	Dynamic block state selection
DC	Direct current
DEAS	Dynamically extended active space
DFT	Density functional theory

DMRG	Density matrix renormalization group
DOS	Density of states
FCI	Full configuration interaction
HF	Hartree-Fock
HOMO	Highest occupied molecular orbital
IRREP	Irreducible representation
LCAO	Linear combination of atomic orbitals
LCC	Local coupled cluster
LMP2	Local second-order Møller-Plesset perturbation theory
LO	Localized orbitals
LT	Localization tensor
LUMO	Lowest unoccupied molecular orbital
MC	Multiconfigurational
MIT	Metal-insulator transition
MoI	Method of increments
MP2	Second-order Møller-Plesset perturbation theory
MPS	Matrix product state
MR	Multireference
MRCC	Multireference coupled cluster
MRCI	Multireference configuration interaction
MRCISD	Multireference configuration interaction singles and doubles
OSV	Orbital specific virtual
PAO	Projected atomic orbital
PES	Potential energy surface

PNO	Pair natural orbital
QIT	Quantum information theory
RAS	Restricted active space
RDM	Reduced density matrix
RG	Renormalization group
RHF	Restricted Hartree-Fock
SA	State average
SCF	Self-consistent field
SD	Slater determinant
SP	Spin-partitioned
SS	Spin-summed
SVD	Singular value decomposition
TISE	Time-independent Schrödinger equation
TPS	Total position-spread
TSCC	Two-state constant-coupling
UHF	Unrestricted Hartree-Fock

Chapter 1

Introduction

Metal-insulator transitions (MITs) are processes that attract particular attention in the condensed-matter physics community[1–8]. This is because the ability to tune the electrical conductivity by changing experimental conditions implies countless practical applications. The pursuit of a complete understanding of the metallic and insulating state has therefore prompted the development of theoretical descriptions based on first principles[9, 10]. This means understanding how the electron transport is affected by electron-nuclei interactions and electron-electron interactions when weak external electric (and/or magnetic) fields are applied. The condition of a small perturbation with the external field is not essential, but it allows the investigation of conducting properties by making considerations based on the analysis of the wave function at thermal equilibrium. This is clearly convenient from a theoretical point of view.

Strictly speaking, the metallic and the insulating states can be meaningfully distinguished only at 0 K. Indeed at finite temperatures thermal excitations cause the direct current (DC) conductivity σ^{DC} of any material to be finite, even if for practical reasons it can be considered negligible for 'insulators'[10, 11]. At absolute zero the distinction is stronger since σ^{DC} vanishes for an insulator while it is finite for a metal. Such a behavior for a metallic state is due to the presence of delocalized electronic states made available by electron-hole excitations at energies immediately above the ground state[10]. However, since the correct description of the electron-hole excitation spectrum is very difficult (if not impossible) for materials of interest, the general theory considers instead the single-electron excitation spectrum to investigate conducting properties. This leads to the well established approximation of the gap criterion[9] according to which the distinctive mark of an insulator is a finite energy gap $\Delta E = (E(n+1) - E(n)) - (E(n) - E(n-1))$ for a system with n electrons. However, this is only a valid approach if the electron-hole excitations can be decoupled into single-electron excitations, or in other words if there is no electron correlation. Indeed, for weakly correlated systems where the driving force of their conducting properties is given by the interaction between electrons and the

periodic potential defined by the nuclei, the analysis of single-electron excitation spectra allows one to make successful predictions. In such situations, a satisfactory description of such a spectrum can be achieved by approximating it with the eigenvalues of an effective one-electron Hamiltonian, that is, via mean-field approaches such as Hartree-Fock (HF) and density functional theory (DFT)[12–16]. Once again, through the analysis of the electronic density of states (DOS) and band structure, insulators can be identified by the presence of a completely filled valence band and a gap in the DOS, while partial filling is characteristic of a metallic behavior[17–19]. Moreover, through the analysis of the gap size, one can evaluate whether thermal excitations can promote an appreciable electrical conductivity at finite temperature, that is, if the material is a semi-conductor[20–23].

The success of such a theory does not only lie in its ability to make such predictions, but maybe more importantly, in the fact that it allows one to design materials with desired transport properties. For instance, the understanding of the band structure allows one to enhance the electrical conductivity by doping the material with specific electron-deficient or electron-rich species[24].

The insulating behavior can be attributed to different phenomena which can be rationalized in terms of an one-electron picture: 1) as already discussed, band insulators are due to a full valence band and a (large) energy gap and therefore the absence of free charge carriers; 2) Peierls insulators[25] present the very same characteristics of the band structure, but the presence of a gap is due to changes in the lattice structure. A typical example of this is dimerized hydrogen chains. As translational symmetry is reduced by the formation of dimers, the Brillouin zone shrinks and the half-filled band splits into a completely filled valence band and an empty conduction band; 3) finally, Anderson insulators[26, 27] are also due to the interaction of electrons with the periodic potential. In these materials, the presence of defects in an otherwise periodic potential causes electrons to be localized and therefore prevent electrical conductivity.

Although the one-electron picture is very successful in many respects, it has to be viewed critically. Drawing conclusions regarding the DC conductivity, which is a two-electron property, from an one-electron picture is an approximation that might break down in presence of strong electron correlation. For instance, gapped systems can behave as superconductors because of the formation of electron pairs at low temperature[10]. Also, the opposite can be true – a variety of materials, such as transition-metal oxides, are poor conductors or even insulators despite having a half filled valence band in an one-electron description[28]. As noted by Rudolf Peierls[29], the strong Coulomb repulsion between electrons is very likely to be responsible for such a behavior, since it causes a reduced electron mobility. These strong electron-correlation effects are ignored by the conventional band-structure model and give rise to a class of insulating materials named Nevill Mott[30–33]. The simplest successful description of Mott insulators and Mott MITs can be obtained by studying the Hubbard Hamiltonian[34–36] which includes the most important terms describing Coulomb correlation of electrons sitting on the same site and the electron hopping between neighbor sites. Although model

Hamiltonians yield satisfactory qualitative descriptions of such phenomena in many cases, many effects are neglected, such as inter-site interactions, multiband effects and orbital degeneracy, which are obviously fundamental for the description of realistic systems[11].

However, disregarding the accuracy of the description of the system, the characterization of the electron transport should be based on the analysis of the ground state wave function only, according to a theory of the insulating state, which is independent to the phenomena driving to the vanishing of the electrical conductivity. Such a theory was proposed by Walter Kohn in his seminal work of 1964[37], where he proved that the insulating behavior can be attributed to the many-body localization of the wave function. This means that the wave function of an insulating system can be written as a sum of many-body Wannier functions which are "localized in disconnected regions of the many-particle configuration space and have essentially vanishing overlap"[37]. This should not be confused with the localization of the electron density in real space which can actually be somewhat delocalized in an insulator[10] (consider for instance covalent insulators).

Much attention has been paid to the analysis of the many-body localization[38–43]. A tool which allows a quantitative measure of this phenomenon is the localization tensor (LT) introduced by Raffaele Resta and co-workers in the late 1990s[44, 45]. The LT, which is given by the second-moment cumulant of the position operator, was shown to be strongly related to the electrical conductivity, since in the thermodynamic limit (that is infinite size) it diverges for metals, while it converges for insulators. Moreover, as further discussed by Souza, Wilkens and Martin[46–48], the connection of the LT with the electrical conductivity was highlighted by its relation with the dielectric polarization which is also a fundamental index of the metallic/insulating character. Directly connected to the localization tensor is the total position-spread (TPS) tensor[49, 50] which applies better than the LT to molecular systems since it is not normalized for the number of electrons. Following the rule of thumb discussed by Resta, in this work the TPS tensor was applied to strongly correlated one-dimensional systems of different sizes in order to study its dependence on the system size and predict the metallic/insulating behavior at the thermodynamic limit. For instance, the TPS was calculated along the dissociation curve of hydrogen chains, which offer a simple quantum-chemical model for the study of MITs (see **Paper m1**). In these systems the electron mobility reduces sensibly when the internuclear distance is stretched, going from a metallic-like state in the bound regime towards an ensemble of non-interacting atoms where charge transfer is clearly impossible. Moreover, just as the electron mobility and therefore the delocalization of the electronic wave function can be studied by means of the TPS tensor, so too can the mobility of α- and β-spin electrons be analyzed by means of a related tool, the spin-partitioned (SP)-TPS tensor. This formalism, which allows deeper insight into the electronic wave function, was introduced and studied in some of the publications composing this work (**Papers m1**, **m2** and **M1**).

Since the electron mobility is strongly dependent on the electron correlation, a satisfactory description of the TPS requires the application of accurate quantum-chemical correlation methods, which, however,

are limited if not unfeasible for extended and periodic systems because of their unfavorable scalings. Therefore as system size grows, alternative approaches to the standard post-Hartree-Fock methods have to be followed. Many efforts have been made to develop sophisticated methods which yield very accurate results for large systems by reducing the Hilbert space according to different strategies. When dealing with periodic systems, local approaches[51–67] are among the most effective methods because of the locality of electron correlation, which can be exploited by choosing a proper representation of the wave function in terms of localized one-electron functions. In this work, among such local approaches, particular focus was given to the method of increments (MoI)[64–68] (see **Papers M3-5**), which yields accurate correlation energies by employing a many-body expansion in terms of localized orbitals. However, the standard formalism of the method of increments cannot provide a smooth ground state dissociation curve. A corrected formalism to do so was then developed and tested in this work (see **Paper M5**). This was critical to describe the change occurring in the systems along the dissociation curve. Furthermore, although the majority of works on this topic focus on the calculation of the correlation energy[69–79], the MoI scheme can be extended in principle to any observable. This was shown by Dolg *et al.*[80, 81] who applied the MoI to the calculations of polarizabilities. In the present work a similar many-body expansion was used for the calculation of the TPS tensor via the MoI.

By using a very different ansatz the density matrix renormalization group (DMRG)[82–91] approach also offers the chance to reduce the computational cost and achieve very accurate results for extended systems. DMRG calculations were then used as a benchmark for testing the applicability of the different formalisms of the method of increments. Furthermore, by applying DMRG, the entanglement analysis achievable by quantum information theory (QIT)[92–101] was exploited for studying MITs (see **Paper M2**). In particular the metallic/insulating character was connected to differences in the decay of the orbital entanglement with distance. Such insight was possible by analyzing the von Neumann entropy and the elements of the two-orbital reduced density matrix which embody information regarding transition probabilities. Moreover, the changes of the block von Neumann entropy with system size were connected to a vanishing energy gap in model systems.

Finally, since entanglement is a key property exploited in the matrix product state (MPS) formalism[90, 91, 102–106] by DMRG, the analysis based on QIT was used to study the effect of a particular one-electron basis on the effectiveness of the DMRG method. As discussed, localized orbitals are less entangled than canonical orbitals and this leads to a substantial improvement of DMRG performance.

This doctoral dissertation is structured as follows: in Chapter 2 a brief insight into the many-electron problem and the standard quantum-chemical electron correlation methods is provided; local methods are introduced in section 2.3 with particular focus on the different formalisms of the method of increments; section 2.4 is dedicated to the density matrix renormalization group, the role played by quantum information theory in DMRG and the entanglement analysis; the chapter concludes

by depicting a mathematical description and highligthing the properties of the TPS tensor and its spin partition (section 2.5); in Chapter 3 a brief description of the systems under study is given. As anticipated, this work focuses on the theoretical investigation of strongly correlated one-dimensional systems. These were chosen to simplify the complexity of the problem and allow the testing of methods under development and tools for the analysis of correlated wave functions; Chapter 4 provides an overlook of the results presented in the scientific publications constituting this work, which are reported in Chapter 5; this dissertation concludes with an outlook presented in Chapter 6.

Chapter 2

Theoretical background

2.1 The many-electron problem

Before diving into the description of the different quantum-chemical methods that have been employed in this work, it is necessary to define a series of terms and concepts for understanding what follows. It is however assumed that the reader is already familiar with key concepts of quantum mechanics such as the idea of wave function, operators and the meaning of the Schrödinger equation, as well as with the Dirac notation.

Let us start by considering the time-independent Schrödinger equation (TISE)[107] for a general molecular system:

$$\hat{\mathcal{H}}_{\mathrm{T}}\Psi(\{x_k\},\{\xi_\kappa\}) = E_{\mathrm{T}}\Psi(\{x_k\},\{\xi_\kappa\}) \tag{2.1}$$

The solution of this eigenvalue problem allows us to evaluate the discrete energy values E_{T} accessible to the system. The full Hamiltonian $\hat{\mathcal{H}}_{\mathrm{T}}$ and the wave function Ψ of an isolated molecular system depend both on the electron coordinates $\{x_k\}$ and the nuclear coordinates $\{\xi_\kappa\}$. As the reader should keep in mind, these involve both spatial and spin coordinates. We will refer to the electronic and nuclear spatial coordinates as $\{r_k\}$ and $\{\rho_\kappa\}$, respectively. Spin variables are indicated as $\{w_k\}$ for electrons and $\{\omega_\kappa\}$ for nuclei.

In our quest for a solution of the TISE we will first apply a brilliant approximation named after Max Born and Robert Oppenheimer[108]. The Born-Oppenheimer approximation (BOA) takes advantage of the fact that the electrons move so much faster than the nuclei that the latter can be considered frozen in comparison to the electronic motion. This adiabatic approximation allows us to factorize the wave function as $\Psi(\{x_k\},\{\xi_\kappa\}) = \Phi(\{x_k\})_{\{\xi_\kappa\}}\Xi(\{\xi_\kappa\})$ where Φ and Ξ are the electronic and nuclear wave function, respectively. Since the Hamiltonian can be also split into an electronic and

nuclear contribution ($\hat{\mathcal{H}}_{\mathrm{T}} = \hat{\mathcal{H}}_{\mathrm{e}} + \hat{\mathcal{H}}_{\mathrm{N}}$), we can define an electronic TISE:

$$\hat{\mathcal{H}}_{\mathrm{e}}\Phi(\{x_k\})_{\{\xi_\kappa\}} = E_{\mathrm{e}}\Phi(\{x_k\})_{\{\xi_\kappa\}} \tag{2.2}$$

This way the BOA leads to a tremendous simplification of Eq. 2.1, since one can focus on the electronic wave function only, in order to calculate the electronic contribution E_{e} to the total energy E_{T}. Moreover, because of this adiabatic approximation, the nuclei have vanishing kinetic energy in the electronic TISE. Therefore only the nuclear repulsion V_{N} contributes to the potential energy within the Born-Oppenheimer approximation.

As it can be seen from Eq. 2.2 Φ depends parametrically on the nuclear coordinates, which have then to be defined before attempting to solve the electronic Schrödinger equation. This means that we can calculate a set of electronic energy eigenvalues for any specified molecular structure. The multidimensional surface describing the dependence of one eigenvalue E_{T} on the nuclear coordinates takes the name of potential energy surface (PES). Although it is important to stress the fact that the PES is an artifact caused by the Born-Oppenheimer approximation, it is a major tool in quantum chemistry since it often allows us to understand chemical processes with a comprehensive description. All methods that will be described in the following sections attempt to solve the electronic time-independent Schrödinger equation by taking advantage of the BOA.

One final consideration has to be made regarding the nature of the electronic Schrödinger equation. As already mentioned, the electronic variables $\{x_k\}$ involve both spatial $\{r_k\}$ and spin variables $\{w_k\}$ which can be decoupled so that $x_k = \{r_k, w_k\}$. A widely employed approximation allows us to omit the spin dependency of the Hamiltonian, which means a non-relativistic Hamiltonian is considered. Relativistic effects which are embodied by the Dirac equation become important when heavy atoms are involved and/or when spin orbital coupling effects need to be described in general. In this work we will not consider such effects, but we will rather always employ a non-relativistic electronic Hamiltonian. In atomic units this has the form

$$\hat{\mathcal{H}}_{\mathrm{e}} = -\frac{1}{2}\sum_k \nabla_k^2 - \sum_k \sum_\kappa \frac{Z_\kappa}{|r_k - \rho_\kappa|} + \frac{1}{2}\sum_k \sum_{j\neq k} \frac{1}{|r_k - r_j|} \tag{2.3}$$

where Z_κ is the charge of the κ^{th} nucleus. The strong electron-electron Coulomb repulsion (third term in Eq. 2.3) causes the electronic motion to be strongly correlated and prevents us from exactly factorizing Φ in terms of one-electron functions. Therefore, despite the simplifications produced by the Born-Oppenheimer approximation and by the use of a non-relativistic Hamiltonian, the electronic TISE is still impossible to solve exactly. This constitutes the many-electron problem, which is probably the main challenge of quantum physics and chemistry. We will explore different methods to obtain approximate solutions for Eq. 2.2 in the following sections, but it is worthwhile to make some

further considerations about Φ which will allow us to evaluate a proper ansatz first. To do so we will analyze the properties that it has to satisfy and describe the nested concepts of quantum states, energy levels, configurations and orbitals.

As mentioned, an (in principle infinite) set of energy eigenvalues E_e can be achieved by solving the electronic Schrödinger equation. These energy values, however, are not sufficient to fully define the state of the system and additional information is required. We can understand this in analogy to the concept of thermodynamic state, which can be fully identified only by the measuring a suitable set of state functions, such as pressure, temperature, volume, etc. In the very same way, in order to unequivocally define a quantum state, one requires the knowledge of a suitable set of observables. Since in quantum mechanics, in order to simultaneously measure different observables, the respective operators must commute with each other, it should be clear that what we are looking for is a complete set of commuting operators (CSCO)[109, 110]. Since we have already defined one of these operators, that is, the Hamiltonian, we need to find operators that commute with it and with each other.

In a general molecular system described by a non-relativistic Hamiltonian, the CSCO are given by the elements of the corresponding symmetry group and the eigenvalues of $\hat{\mathbb{S}}^2$ and $\hat{\mathbb{S}}_z$ spin operators, $s(s+1)$ and s_z. In other words, the knowledge of the irreducible representation (IRREP) Γ according to which the wave function transforms as well as the spin quantum numbers s and s_z of the full system and the corresponding energy eigenvalue gives us full information about the quantum state of the system.

Because of spatial and spin symmetry different states are energetically degenerate. In particular for a specified s quantum number, $2s+1$ degerate states with $s_z = s, s-1, \cdots, -|s-1|, -s$ are expected. Similarly, states transforming according to a m-dimensional IRREP will be part of a m-fold set of degenerate states. All states which are degenerate as a consequence of this relations will constitute an energy level, which according to the general convention will be labeled as ${}^{2s+1}\Gamma$.

It has to be underlined that atoms and linear molecules are special cases since their CSCOs comprehend additional operators. In particular for atoms, because of their spherical symmetry, the squared total electronic orbital angular momentum $\hat{\mathcal{L}}^2$ and one of its components (in general the z component $\hat{\mathcal{L}}_z$ is considered) should be defined. For linear molecules instead the net electronic orbital angular momentum along the bond axis has to be considered.

Besides allowing us to define correctly a quantum state, the knowledge of these properties will help when writing a proper ansatz for the electronic wave function. Since an analytical form of Φ cannot be achieved, we can write the exact wave function as a linear combination of a proper complete set of n-electron functions $\{\phi_i\}$:

$$|\Phi\rangle = \sum_i c_i \, |\phi_i\rangle \tag{2.4}$$

Knowing the properties that Φ must satisfy allows us to make a mindful selection of $\{\phi_i\}$. Indeed, we can safely state that the corresponding expansion coefficients c_i will not vanish if they are eigenfunctions of the CSCO with the same eigenvalues as Φ. We require, therefore, an expression for these 'building blocks' of the wave function, which respect these properties.
Maybe the most intuitive expression for these n-electron functions is the product of n one-electron functions $\{\chi_\mu\}$, *i.e.* a Hartree product. This form however does not respect one further property of the electronic wave function, that is, that it must be antisymmetric with respect to the exchange of any two electrons. In formulas:

$$\Phi(x_1 \cdots x_p \cdots x_z \cdots x_n) = -\Phi(x_1 \cdots x_z \cdots x_p \cdots x_n) \tag{2.5}$$

The antisymmetrized products of one-electron functions are named after John C. Slater, who in 1929 introduced the idea of using determinants in order to describe the wave function[111], even if such form had already been employed by Werner K. Heisenberg[112] and Paul Dirac[113]. A Slater determinant (SD), which by definition respects the required antisymmetry and consequently the Pauli principle, has the form:

$$|\phi_{\mathrm{SD}}\rangle = \frac{1}{\sqrt{n!}} \begin{vmatrix} \chi_1(x_1) & \chi_2(x_1) & \cdots & \chi_n(x_1) \\ \chi_1(x_2) & \chi_2(x_2) & \cdots & \chi_n(x_2) \\ \vdots & \vdots & \ddots & \vdots \\ \chi_1(x_n) & \chi_2(x_n) & \cdots & \chi_n(x_n) \end{vmatrix} \tag{2.6}$$

It is often the case that a single Slater determinant might not be an eigenfunction of all CSCO. However by applying symmetry, proper linear combinations of Slater determinants can always be made which yield a proper set of $\{\phi_i\}$. We will refer to them as configuration state functions (CSFs). The one-electron functions $\{\chi_\mu\}$ are denoted as spin orbitals, a term that derives from analogy with the one-electron functions which are exact solutions of the TISE for the hydrogen atom. For a non-relativistic Hamiltonian, spin orbitals can be factorized in terms of a spatial function and a spin function which can assume two values only, corresponding to spin-up (α) or spin-down (β):

$$\chi_\mu(x) = \varphi_\nu(r)\sigma(w) \qquad \text{with} \qquad \sigma(w) = \alpha, \beta \tag{2.7}$$

The spatial orbitals (or simply orbitals) $\{\varphi_\nu\}$ can then host up to two electrons with opposite spin and are often used in many formalisms instead of spin orbitals.
By choosing a specific distribution of n electrons into orbitals, we can identify one electronic configuration of the molecular or atomic system. Although arguments based on electronic configurations are often used to make simple interpretations of chemical phenomena, we should keep in mind that

they are based on a one-electron description and they should never be confused with the concept of electronic state.

To conclude, a set of one-electron functions is required in order to construct all possible Slater determinants and in turn CSFs and the exact wave function through linear combinations. Before describing how to obtain the 'best' possible set of orbitals, we must first introduce a further keystone concept of quantum chemistry which is used in many methods to approximately solve the TISE. That is the variational principle. This states that for any trial-approximated ground-state wave function $\tilde{\Phi}_0$, the expectation value of the Hamiltonian is always larger than or equal to the energy of the ground state, E_0:

$$\frac{\langle \tilde{\Phi}_0 | \, \hat{\mathcal{H}}_\mathrm{e} \, | \tilde{\Phi}_0 \rangle}{\langle \tilde{\Phi}_0 | \tilde{\Phi}_0 \rangle} \geq E_0 \tag{2.8}$$

We will see in the next section how the presence of this lower boundary for the energy is exploited in different quantum-chemical methods, to which we will refer as variational methods. As stated above, Eq. 2.4 yields the exact wave function if a complete set of n-electron functions is used. This means an infinite set, which in turn requires an infinite amount of one-electron functions, which is unfeasible for obvious reasons. Any wave function obtained by applying a truncation in Eq. 2.4 will respect the variational principle (Eq. 2.8).

2.2 Standard quantum-chemical methods

2.2.1 Hartree-Fock

Considering what we have explained so far, it should be clear how the lowest level of approximation for an electronic wave function can be achieved with a single CSF. The method developed by Douglas Hartree and Vladimir Fock at the end of the 1920s[114, 115] is based on such an approximated ansatz of the wave function and exploits a self-consistent algorithm which minimizes the energy by optimizing the occupied orbitals. The cornerstone of the Hartree-Fock method is that it defines an effective one-electron Hamiltonian, the Fock operator, whose eigenfunctions are the canonical orbitals. In this brief description of the HF method, we will use spin orbitals. However, the reader should note that an analogous formalism can be derived by using spatial orbitals and imposing spin orbitals corresponding to the same $\varphi(r)$ to be degenerate. This leads to the restricted HF (RHF). In the unrestricted HF (UHF)[116] further degrees of freedom are added, by allowing all spin orbitals to optimize independently.

The Fock equations

In the following, for sake of simplicity we will consider a CSF consisting of a single Slater determinant. We will start by the expression of the expectation value of the energy for a SD of the form of Eq. 2.6 with orthonormal spin orbitals:

$$E_{\mathrm{SD}} = \sum_k \langle \chi_k | \hat{h} | \chi_k \rangle + \sum_k \sum_{j \neq k} \langle \chi_k \chi_j | \hat{g} | \chi_k \chi_j \rangle - \langle \chi_k \chi_j | \hat{g} | \chi_j \chi_k \rangle \begin{cases} \hat{h} = -\frac{1}{2}\nabla_k^2 - \sum_\kappa \frac{Z_\kappa}{|r_k - \xi_\kappa|} \\ \hat{g} = \frac{1}{|r_k - r_j|} \end{cases} \tag{2.9}$$

where the summation indices k and j run over the spin orbitals present in the Slater determinant. Because of the variational principle, E_{SD} has as lower bound the exact energy E_0. We can therefore minimize it with respect to small variations of the spin orbitals under the constraint of mutual orthogonality. This can be achieved by use of the Lagrange multiplier method:

$$\frac{\partial E_{\mathrm{SD}}}{\partial \chi_k} - \frac{\partial}{\partial \chi_k} \sum_k \sum_j \lambda_{kj} (\delta_{kj} - \langle \chi_k | \chi_j \rangle) = 0 \tag{2.10}$$

where the scalars λ_{kj} are the Lagrange multipliers and δ_{kj} is a Kronecker-delta. By solving the set of n equations defined by Eq. 2.10 one obtains:

$$\hat{\mathcal{F}} | \chi_k \rangle = \sum_j \lambda_{kj} | \chi_j \rangle \tag{2.11}$$

where $\hat{\mathcal{F}}$ is the Fock operator. There always exists a proper unitary transformation of the orbitals $\{\chi_k\} \rightarrow \{\tilde{\chi}_k\}$ which allows us to express this equation as:

$$\hat{\mathcal{F}}|\tilde{\chi}_k\rangle = \varepsilon_k|\tilde{\chi}_k\rangle \tag{2.12}$$

The Fock equation, Eq. 2.12, is of extreme importance, because it states that if the wave function is described by a single determinant ansatz, there exists a set of optimal orthonormal orbitals $\{\tilde{\chi}_k\}$ which minimize the energy and have the incredible property of being eigenfunctions of an effective one-electron Hamiltonian, $\hat{\mathcal{F}}$, with eigenvalues ε_k.
In order to understand how the optimization works, it is worthwhile to describe first the structure of the Fock operator, which is generally split into three terms, the one-electron operator $\hat{h}$ and the two electron Coulomb $\hat{\mathcal{J}}$ and exchange $\hat{\mathcal{K}}$ operators:

$$\hat{\mathcal{F}} = \hat{h} + \hat{\mathcal{J}} + \hat{\mathcal{K}} \tag{2.13}$$

where the latter two operators depend on the orbitals themselves:

$$\hat{\mathcal{J}} = \sum_j \hat{\mathcal{J}}_j \qquad \text{with} \qquad \hat{\mathcal{J}}_j\tilde{\chi}_k = \int \tilde{\chi}_j^*(x')\frac{1}{|r'-r|}\tilde{\chi}_j(x')\tilde{\chi}_k(x)dx'dx \tag{2.14}$$

$$\hat{\mathcal{K}} = \sum_j \hat{\mathcal{K}}_j \qquad \text{with} \qquad \hat{\mathcal{K}}_j\tilde{\chi}_k = \int \tilde{\chi}_j^*(x')\frac{1}{|r'-r|}\tilde{\chi}_k(x')\tilde{\chi}_j(x)dx'dx \tag{2.15}$$

Because of this dependence the Hartree-Fock method requires a self-consistent field (SCF) approach. This means that we will start from an approximated form for $\{\tilde{\chi}_k\}$, construct the Fock operator and solve the Fock equations to determine a new set of spin orbitals. New iterations are then repeated until convergence is reached.

One-electron basis sets and the Roothan-Hall equations

Clearly, in order to optimize the orbitals by solving the Fock equation, a set of degrees of freedom needs to be selected first. Very accurate results can be obtained by the use of numerical methods which allow the optimization of the orbitals on a three-dimensional grid which discretizes the $\{r_k\}$ which are continuous in $\mathbb{R}^3$. However, in order to reduce the computational cost, most methods exploit analytical basis sets. This means that each orbital is expanded as a linear combination of a set of functions which constitute a one-electron basis set and the expansion coefficients are used as optimization parameters. Different functions can be employed, but because they strongly simplify the evaluation of one- and two-electron integrals, Gaussians are the widest used in quantum-chemical methods. The use of such functions leads us to another key point of quantum chemistry, that is the use

of a linear combination of atomic orbitals (LCAO) as an ansatz for molecular orbitals. These atomic orbitals can in turn be described by linear combinations of atom-centered Gaussians.
By expanding the canonical orbitals in terms of a one-electron basis set, the Fock equations can finally be expressed in matrix form, which constitutes the Roothan-Hall equation[117, 118]:

$$\mathbf{F}\mathbf{C}_{\mathrm{MO}} = \mathbf{S}\mathbf{C}_{\mathrm{MO}}\boldsymbol{\mathcal{E}} \tag{2.16}$$

In Eq. 2.16, $\mathbf{F}$ is the Fock matrix, $\mathbf{S}$ the overlap matrix, the $\mathbf{C}_{\mathrm{MO}}$ matrix contains the coefficient used to expand the molecular orbitals in term of the one-electron basis set and $\boldsymbol{\mathcal{E}}$ is the diagonal matrix whose elements are the orbital energies ε_k.

Final considerations

The direct consequence of employing a single Slater determinant is that a mean field approximation is implicitly introduced. Indeed, in our attempt to factorize the n-electron wave function in terms of n one-electron functions, we are implying that the probability of finding one electron in a particular region of space is independent of the position of the electrons with the opposite spin, that is they are uncorrelated. Indeed, the Coulomb repulsion between electrons is averaged since the Fock operator considers the interaction between each fermion and the density created by the others. The missing contribution to the energy of the system is referred to as correlation energy.
We have to stress the fact, however, that although the HF method is generally referred to as an uncorrelated method, this is misleading since electrons with same spins are actually partially correlated thanks to the Pauli principle, which is taken into account by the Slater determinant ansatz itself. This is described by the exchange integrals. Nevertheless, we will refer to correlation energy E_{corr} when describing the difference between the exact energy and the Hartree-Fock energy.
In order to calculate the correlation energy, we will apply more sophisticated methods using the Hartree-Fock wave function as the starting point. Indeed, as already mentioned in section 2.1, we will attempt to approximate the exact wave function by generating all (or as many as) possible configuration state functions by using the canonical orbitals obtained via the HF method. For this reason, these methods are generally referred as post-Hartree-Fock methods.
Finally, we want to stress the fact that the dimension D of the one-electron basis set corresponds to the number of orbitals that can be generated, but HF optimizes only the n spin orbitals included in Slater determinant. Therefore a distinction emerges between the n occupied canonical spin orbitals and the $D - n$ virtual spin orbitals. Although the latter are an artifact of the use of a one-electron basis set and they have no real physical meaning, the difference between the eigenvalue of the lowest unoccupied molecular orbital (LUMO) and the highest occupied molecular orbital (HOMO) are often used as an approximated evaluation of the excitation gap according to the Koopmans' theorem[119].

Moreover, the virtual orbitals play a fundamental role in post-Hartree-Fock methods. Indeed, once the Fock equations have been solved, one can construct a variety of configuration state functions just by defining excitations from the ground CSF into the virtual space. The so generated n-electron functions have the advantage of being orthogonal to each other and span a subspace of the infinite Hilbert space where the exact wave function is defined, the Fock space.

2.2.2 Configuration interaction

In light of the explanations of section 2.2.1, it should be clear how we can approximately expand the exact wave function as in Eq. 2.4, where all $\{\phi_i\}$ are constructed by starting from the HF CSF by performing excitations into the virtual space. If we insert this ansatz in the electronic TISE we obtain:

$$\hat{\mathcal{H}}_{\mathrm{e}} |\Phi\rangle = E_{\mathrm{e}} |\Phi\rangle \tag{2.17}$$

$$\sum_i c_i \hat{\mathcal{H}}_{\mathrm{e}} |\phi_i\rangle = E_{\mathrm{e}} \sum_i c_i |\phi_i\rangle \tag{2.18}$$

By multiplying both sides for $\langle\phi_j|$ and exploiting orthonormality relations:

$$\sum_i c_i \langle\phi_j| \hat{\mathcal{H}}_{\mathrm{e}} |\phi_i\rangle = E_{\mathrm{e}} c_j \tag{2.19}$$

This equation can be expressed in matrix form (Secular equation):

$$\mathbf{HC} = \mathbf{EC} \tag{2.20}$$

where $\mathbf{H}$ is the Hamiltonian matrix in the $\{\phi_i\}$ basis, $\mathbf{C}$ the coefficient matrix and the diagonal matrix $\mathbf{E}$ contains the eigenvalues of the electronic Hamiltonian.
It has to be underlined that $\mathbf{H}$ is actually a very sparse matrix. Indeed, since the Hamiltonian is a two-electron operator, according to the Slater-Condon rules[111, 120] the only non-vanishing elements H_{ij} are those where ϕ_i and ϕ_j differ by single and double excitations. A further element of sparseness arises as a direct consequence of employing canonical orbitals. Indeed, since they are eigenfunctions of an effective one-electron operator, the Fock operator, it can be shown that any element which involves the Hartree-Fock CSF and a single excited CSF is also zero. This property is described by the Brilluoin theorem[121].
Once the elements of $\mathbf{H}$ are constructed employing one-electron and two-electron integrals, the only remaining task is to diagonalize this matrix in order to obtain all possible eigenvalues of $\hat{\mathcal{H}}$. The method that we have described so far goes under the name of Full Configuration Interaction (FCI) and if applied would give us the best achievable answer to the many-electron problems, within the limit of the one-electron basis set employed and the BOA, of course. However, despite the relatively simple construction of the Hamiltonian matrix, its factorial growth with system and one-electron basis set size soon makes storage and diagonalization unfeasible. This frustrating reality of the many-electron problem led to the development of a variety of faster and more efficient approaches which overcome the dimensionality problem. We will begin by analyzing the most fundamental of these which consists of a truncation of the configuration interaction (CI) wave function (Eq. 2.4) and will then discuss more

sophisticated methods, such as coupled cluster and the more recent density matrix renormalization group, describing both their advantages and disadvantages.

Truncated CI

The most obvious solution for reducing the size of the Hamiltonian matrix is to cut down the amount of CSFs involved by including only low-level excitations, such as single and double excitations. Indeed, these are likely to be the ones which affect the character of the wave function the most. Moreover, since only CSFs related by double excitations yield non-vanishing elements it seems also more reasonable that they should be the most important for inclusion in the expansion of the wave function. Indeed, from Eq. 2.19, if a pre-normalized wave function is considered ($c_{\mathrm{HF}} = 1$), the FCI correlation energy can be expressed as:

$$E_{\mathrm{corr}} = \sum_{\substack{a,b \\ \alpha,\beta}} c_{ab}^{\alpha\beta} \langle \phi_{\mathrm{HF}} | \hat{\mathcal{H}}_{\mathrm{e}} | \phi_{ab}^{\alpha\beta} \rangle \tag{2.21}$$

where $|\phi_{ab}^{\alpha\beta}\rangle$ is the CSF obtained by double excitation from the HF occupied orbitals a and b into the virtual orbitals α and β. Independently of the level of truncation of the CI wave function, the correlation energy will be expressed as in Eq. 2.21. However, it should be clear that the values of the coefficient will be strongly affected, although the matrix elements of $\hat{\mathcal{H}}$ will not. Nevertheless, for many small systems a CI singles and doubles (CISD) will give an acceptable level of approximation with respect to FCI, as long as we are not interested in describing dissociation processes. Indeed, truncated CI wave functions suffer a lack of a very important requirement of the electronic wave function, size-extensivity[122, 123]. This is the formal condition of correct scaling that a method should satisfy. To understand this, let us consider the wave function describing a collection of non-interacting fragments. The corresponding energy should be equal to the sum of the energies of the individual fragments. In other words, a method is size-extensive, if the calculated energy scales linearly with the number of electrons in the non-interacting limit.

The apparently simple requirement of size-extensivity is not easy to satisfy if a truncated CI is employed. Say that a single fragment can be described by means of CISD. In this case, in order to achieve the same level of approximation for describing two non-interacting fragments, up to quadruple excitations should be included. The error caused by lack of size-extensivity might be rather large and becomes more and more important as the system size increases. A way of correcting truncated CI results is to apply an ad-hoc correction to the energy ΔE_Q given by the Davidson correction[124, 125], calculated as:

$$\Delta E_Q = \frac{(1 - c_{\mathrm{HF}}^2)}{c_{\mathrm{HF}}^2} (E_{\mathrm{CISD}} - E_{\mathrm{HF}}) \tag{2.22}$$

As soon as the weight of the HF configuration c_{HF} is large (that is, the correction is small), this approach yields reliable results. However, far more sophisticated approaches exist that include size-extensivity in the ansatz of wave function without need for further corrections. Among those, probably the most efficient approach that allows us to achieve FCI-like size-extensive results is the coupled cluster.

2.2.3 Coupled cluster

As we have seen, the linear expansion used so far to describe the wave function leads to a system of linear equations involving the energy and the expansion coefficients (Eq. 2.19). In order to reduce to number of equations a truncated CI has to be employed, but this leads to a lack of size-extensivity. We will see in this section how, by employing a different ansatz, the coupled cluster method allows us to solve the TISE without this drawback by employing a set of non-linear equations whose size is the same as of a truncated CI.

Let us start by rewriting the FCI wave function in terms of excitation operators $\hat{\mathfrak{T}}_{ab\ldots z}^{\alpha\beta\ldots\omega}$, where $ab\ldots z$ are occupied orbitals in the HF CSF, ϕ_{HF}, and $\alpha\beta\ldots\omega$ are virtual orbitals. By acting on ϕ_{HF}, these operators generate excited CSFs $\phi_{ab\ldots z}^{\alpha\beta\ldots\omega}$ multiplied by the respective amplitudes[1] $t_{ab\ldots z}^{\alpha\beta\ldots\omega}$ yielding an expression equal to Eq. 2.4:

$$
\begin{aligned}
|\Phi_{\mathrm{FCI}}\rangle &= \left(1 + \sum \hat{\mathfrak{T}}_a^\alpha + \sum \hat{\mathfrak{T}}_{ab}^{\alpha\beta} + \sum \hat{\mathfrak{T}}_{abc}^{\alpha\beta\gamma} + \cdots\right) |\phi_{\mathrm{HF}}\rangle && (2.23)\\
&= |\phi_{\mathrm{HF}}\rangle + \sum t_a^\alpha |\phi_a^\alpha\rangle + \sum t_{ab}^{\alpha\beta} |\phi_{ab}^{\alpha\beta}\rangle + \sum t_{abc}^{\alpha\beta\gamma} |\phi_{abc}^{\alpha\beta\gamma}\rangle + \cdots && (2.24)
\end{aligned}
$$

The key point of couple cluster (CC)[126–132] theory is the use of a different ansatz where the cluster operator $\hat{\mathfrak{T}} = \sum \hat{\mathfrak{T}}_{ab\ldots z}^{\alpha\beta\ldots\omega}$ does not act linearly, but rather exponentially on ϕ_{HF}. As one can easily verify, it is remarkable that the resulting expression involves the same CSFs included in the FCI wave function, no matter which level of excitations is included in $\hat{\mathfrak{T}}$. Consider for instance only single excitations:

$$
\begin{aligned}
|\Phi_{\mathrm{CCS}}\rangle &= \mathrm{e}^{\hat{\mathfrak{T}}} |\phi_{\mathrm{HF}}\rangle && (2.25)\\
&= \left(1 + \hat{\mathfrak{T}} + \frac{1}{2!}\hat{\mathfrak{T}}^2 + \frac{1}{3!}\hat{\mathfrak{T}}^3 + \cdots\right) |\phi_{\mathrm{HF}}\rangle && (2.26)\\
&= \left(1 + \sum \hat{\mathfrak{T}}_a^\alpha + \frac{1}{2!}\sum \hat{\mathfrak{T}}_a^\alpha \hat{\mathfrak{T}}_b^\beta + \frac{1}{3!}\sum \hat{\mathfrak{T}}_a^\alpha \hat{\mathfrak{T}}_b^\beta \hat{\mathfrak{T}}_c^\gamma + \cdots\right) |\phi_{\mathrm{HF}}\rangle && (2.27)
\end{aligned}
$$

Even at the CC singles (CCS) level, the Taylor expansion of the cluster operator creates all singles, doubles, triples, etc. which insure a size-extensive wave function. In this particular case where the amplitudes of the higher excited CSFs depend on those of the singles (for instance $t_{ab}^{\alpha\beta} = t_a^\alpha t_b^\beta$), the higher excitations are called disconnected. Because of this, the flexibility of Φ_{CCS} is not comparable to Φ_{FCI}, but the inclusion of connected doubles $\hat{\mathfrak{T}}_{ab}^{\alpha\beta}$ and triples $\hat{\mathfrak{T}}_{abc}^{\alpha\beta\gamma}$ into the cluster operator is in general enough to achieve a results comparable to FCI.

Despite the fact that, because of the exponential ansatz, size-extensivity is preserved independently of the truncation of the cluster operator, so far this does not seem to have brought any advantage in the

[1] In coupled cluster formalism we refer to the expansion coefficients as amplitudes.

solution of the TISE:

$$\hat{\mathcal{H}}_{\mathrm{e}}\mathrm{e}^{\hat{\mathcal{T}}}\left|\phi_{\mathrm{HF}}\right\rangle = E_{\mathrm{e}}\mathrm{e}^{\hat{\mathcal{T}}}\left|\phi_{\mathrm{HF}}\right\rangle \tag{2.28}$$

If we had to solve it in an analogous way to Eq. 2.19, that is by projecting on all the $\langle\phi_{ab\ldots z}^{\alpha\beta\ldots\omega}|$ we would run into an infinite series. Instead, the mathematics of exponentials allows us to obtain an alternative set of equations by means of the Baker-Campbell-Hausdorff (BCH) formula:

$$\mathrm{e}^{-\hat{\mathcal{T}}}\hat{\mathcal{H}}_{\mathrm{e}}\mathrm{e}^{\hat{\mathcal{T}}} = \hat{\mathcal{H}}_{\mathrm{e}} + [\hat{\mathcal{H}}_{\mathrm{e}},\hat{\mathcal{T}}] + \frac{1}{2!}[[\hat{\mathcal{H}}_{\mathrm{e}},\hat{\mathcal{T}}],\hat{\mathcal{T}}] + \frac{1}{3!}[[[\hat{\mathcal{H}}_{\mathrm{e}},\hat{\mathcal{T}}],\hat{\mathcal{T}}],\hat{\mathcal{T}}] + \frac{1}{4!}[[[[\hat{\mathcal{H}}_{\mathrm{e}},\hat{\mathcal{T}}],\hat{\mathcal{T}}],\hat{\mathcal{T}}],\hat{\mathcal{T}}] \tag{2.29}$$

According to the BCH formula, the transformed Hamiltonian $\mathrm{e}^{-\hat{\mathcal{T}}}\hat{\mathcal{H}}_{\mathrm{e}}\mathrm{e}^{\hat{\mathcal{T}}}$ can be exactly expressed by a finite series which is at the worst quartic for $\hat{\mathcal{T}}$. By employing the relation $\langle\phi_{\mathrm{HF}}|\,\mathrm{e}^{-\hat{\mathcal{T}}} = \langle\phi_{\mathrm{HF}}|$, this allows us to obtain a new set of equations for the amplitudes, by projecting on the connected excited CSFs. In the case of CCSD (CC singles and doubles), the so obtained coupled cluster equations are:

$$\langle\phi_{\mathrm{HF}}|\,\mathrm{e}^{-\hat{\mathcal{T}}}\hat{\mathcal{H}}_{\mathrm{e}}\mathrm{e}^{\hat{\mathcal{T}}}\left|\phi_{\mathrm{HF}}\right\rangle = E_{\mathrm{e}} \tag{2.30}$$

$$\langle\phi_{a}^{\alpha}|\,\mathrm{e}^{-\hat{\mathcal{T}}}\hat{\mathcal{H}}_{\mathrm{e}}\mathrm{e}^{\hat{\mathcal{T}}}\left|\phi_{\mathrm{HF}}\right\rangle = 0 \tag{2.31}$$

$$\langle\phi_{ab}^{\alpha\beta}|\,\mathrm{e}^{-\hat{\mathcal{T}}}\hat{\mathcal{H}}_{\mathrm{e}}\mathrm{e}^{\hat{\mathcal{T}}}\left|\phi_{\mathrm{HF}}\right\rangle = 0 \tag{2.32}$$

It is remarkable that the energy appears in only the first of the CC equations. This decoupling allows us to solve the other equations first in order to evaluate the amplitudes and then use them to calculate the energy.

CCSD constitutes a good compromise between computational cost and accuracy. In those situation where the description of triples or higher excitation become necessary, instead of employing CCSDT or CCSDTQ, one can achieve excellent solutions by means of a computationally cheaper approach. This consists of using the doubles' amplitudes to calculate approximate second order triples' amplitudes via perturbation theory, which are in turn used to derive corrections to the energy. The described method is referred to as CCSD(T)[133–135] and is maybe the most commonly employed coupled cluster method.

Final considerations

We conclude the description of CC with some final comments. As the reader might have already noticed, the coupled cluster equations are not derived by invoking the variational principles. This is because minimizing the expectation value of the energy $\frac{\langle\phi_{\mathrm{HF}}\mathrm{e}^{\hat{\mathcal{T}}^{\dagger}}\hat{\mathcal{H}}_{\mathrm{e}}\mathrm{e}^{\hat{\mathcal{T}}}\phi_{\mathrm{HF}}\rangle}{\langle\phi_{\mathrm{HF}}\mathrm{e}^{\hat{\mathcal{T}}^{\dagger}}\mathrm{e}^{\hat{\mathcal{T}}}\phi_{\mathrm{HF}}\rangle}$ would lead to an intractable set of nonlinear equations. Coupled cluster is not a variational method and although the method is very accurate, it might yield energy lower than FCI. The drawback of the CC approach is however not the lack of variationality, but rather the fact that it is a single-reference method, that is, it uses the HF

CSF as a reference. Therefore coupled cluster fails in those situations where HF does not yield a good description of the system. As we will see in section 2.2.4, in these situations references consisting of more CSFs (multiconfigurational) have to be obtained, so that multireference methods can be applied. Following the assumption that a large multireference character implies large values of the amplitudes of excited determinants, useful diagnostics based on the analysis of such coefficients give the chance of evaluating whether the CC results can be considered reliable. In particular the $\mathcal{T}_1$ diagnostic[136] considers the norm of the single excited vector $|t(1)|$ normalized by the number of electrons n:

$$\mathcal{T}_1 = \frac{|t(1)|}{\sqrt{n}} \tag{2.33}$$

Coupled cluster results are in general considered reliable is $\mathcal{T}_1$ is smaller than 0.02-0.025.

2.2.4 Multiconfigurational self-consistent field and multireference methods

As already stated, single-reference methods work reliably for all those situations where a single CSF is a physically acceptable minimal description of the wave function. This however is often not the case. Typical examples are open shell atoms with valence p or d orbitals for which the ground configuration gives rise to a variety of states each composed of a linear combination of CSFs. All the orbitals constituting these Slater determinants need to be optimized together which, as we know, HF is not capable of.

The approach capable of dealing with such a problem is the multiconfigurational self-consistent field (MC-SCF) method. The expression of the MC-SCF wave function is not different from the CI wave function (see 2.4), but the expansion spans a limited part of the Fock space. The n-electron functions constituting a MC-SCF wave function are constructed by performing excitations within a particular set of one-electron functions, the active orbitals. MC-SCF does not involve a direct diagonalization of the Hamiltonian, but rather a SCF cycle which invokes the variational principle in order to minimize the energy by optimizing both the CI coefficients and the active orbitals.

The one-electron picture that emerges from the HF method is completely lost in such a treatment. Indeed, the optimized active orbitals are not eigenfunctions of an effective Hamiltonian such as the Fock operator, and their associated energy does not have a particular physical meaning as for the canonical orbitals. However, these functions are extremely important since they diagonalize the one-electron density matrix and therefore allow us to write the wave function in the most compact form possible, by employing the smallest possible number of CSFs. These functions are called natural orbitals and, because of this intrinsic property, they play a key role in multireference (MR) calculations performed on top of a MC-SCF wave function.

Obviously, a multiconfigurational wave function contains some of the electron correlation. Even if a well marked distinction is hard to make, the correlation energy described by including the necessary nearly-degenerate CSFs at the MC-SCF level of theory is called static in contrast to the dynamical correlation. The latter is the correlation of the movement of electrons and can be described by methods such as configuration interaction and coupled cluster.

It of course clear, that since both CI and orbital coefficients are optimized, only a restricted amount of configurations can be included in the calculations. Various choices can be made concerning the active space employed in a MC-SCF and often a careful analysis of the chemical problem has to be made in advance to choose the orbitals to include, making MC-SCF often difficult to apply. The complete active space (CAS)-SCF[137–139] constitutes maybe the widest employed approach since it reduces the work needed to select the active orbitals and constructs all possible CSFs which can be generated with those. If the CAS is not feasible, other choices might be necessary for reducing the active space. For example, the active orbitals can be divided into different subsets and restrictions on the order of

excitations from/to some of these can be forced. This approach is referred to as restricted active space (RAS)-SCF. In the general nomenclature CAS(n,m) or RAS(n,m) indicate MC-SCF calculations involving n active electrons in m active orbitals.

So far we have considered MC-SCF calculations applied in order to minimize the energy of the ground-state only. However, it is often the case that multiple states have to be optimized simultaneously. Indeed, the natural orbitals obtained by a MC-SCF performed on a single state only might not be a proper choice for successive multireference calculations on excited states. This is also a problem that has to be dealt with in systems presenting a large number of low energy states such as d-metal complexes, even if one is interested in the ground state only. The state-averaged (SA) MC-SCF offers to chance of performing such a mutual optimization by minimizing a properly defined energy functional which depends on the energy of all considered states. In a sense SA natural orbitals are a better mathematical choice for successive MR calculations, which are necessary to include dynamical correlation and obtain meaningful approximations to energy eigenvalues.

In analogy to CI calculations performed on top of HF wave functions, multireference CI (MRCI)[140, 141] calculations can be performed on top of MC wave functions. Although the equations involved become more cumbersome, the concept behind the methods is the same. This means that we will construct single and double (or higher) excited determinants from the reference CSFs which constitute the MC wave functions. As in the case of single-reference CI, size-extensive corrections such as Davidson's have to be applied by employing algorithms similar to those seen in section 2.2.2. In this work, we applied MRCISD (MRCI singles and doubles) and a more sophisticated size-extensive MRCI approach, the averaged coupled pair functional (ACPF)[142]. This takes care of the lack of size-extensivity by inserting corrections in the diagonal elements of the Hamiltonian matrix before diagonalization. Finally, the CC equations can be applied on top of a multiconfigurational wave function, too[143–145]. However, the equations to be solved are rather cumbersome and hard to handle. Therefore MRCC methods have only been implemented in a few codes so far.

2.2.5 Considerations about standard quantum-chemical methods

Scaling

In the discussion of standard quantum-chemical methods the reader was often warned that according to system size $\mathcal{N}$, some methods are unfeasible. A desirable property of a method would be a low order (or even linear) scaling, that is, the computational cost should increase at low rate as the number of electrons and basis functions grows. For instance the HF method, for which the bottleneck is given by the integral storage, scales upmost as $\mathcal{O}(\mathcal{N}^4)$, while correlation methods have more unfavourable scalings ranging from $\mathcal{O}(\mathcal{N}^5)$ for MP2 (second-order Møller-Plesset perturbation theory[146]), $\mathcal{O}(\mathcal{N}^6)$ for CCSD and $\mathcal{O}(\mathcal{N}^7)$ for CCSD(T) up to $\mathcal{O}(\mathcal{N}!)$ for FCI.
Smart implementations, such as the use of density fittings[147, 148], can reduce such scalings and what were considered impossible problems a few decades ago are now routine calculations, thanks to the continuous advances in computer science. Nevertheless, when dealing with extended systems, wave function correlation methods are often still not a feasible option and DFT is generally employed instead. Therefore there is great interest in the development of new wave-function based approaches to overcome this dimensionality issue. We will describe two such approaches in the next sections, the method of increments, which is one variant of the local correlation methods, and the density matrix renormalization group.

Size-consistency

Some further considerations have to be made about a concept which is often confused and used interchangeably with size-extensivity, size-consistency. While as already described in section 2.2.2, size-extensivity refers to the correct scaling of the energy with the number of electrons, the concept of size-consistency, introduced by Pople[149], is connected to the description of fragmentation. Stated clearly, it is the requirement that a dissociation curve of a specific state be described without discontinuities using the same ansatz for the wave function for any molecular structure. For instance, a ground-state dissociation curve is described in a size-consistent manner at the HF level if the employed ground-state CSF involves the same orbitals from the bound regime till dissociation.
In contrast to size-extensivity, size-consistency is not a property of the method itself, but depends rather on the process under study. As an example, RHF is a size-extensive method, but depending on the process it might not yield size-consistent results. Therefore single-reference methods can be affected by a lack of size-consistency if they are performed on top of a size-inconsistent HF reference. On the other hand, this problem is not in general encountered for multireference methods if the active space used in MC-SCF reference was properly chosen. This simple statement is very important because it underlines the importance of the reference wave function for obtaining meaningful results.

This considerations regarding the relation between a reference and size-consistency will be very important when discussing how dissociation curves can be described via local methods.

2.3 Local correlation methods

In this section we will give a brief overview of the local methods with a focus on the method of increments (MoI). The crucial point of these approaches is that they exploit the short range nature of electron correlation. So far, we have employed different truncations of Eq. 2.4 based on excitations in a canonical orbital representation. Although these are undoubtedly strong arguments, truncations based on a distance criterion can often yield high-quality results comparable to the ones of standard correlation methods. Moreover, because of the reduced scaling, local approaches allow us to treat systems which are prohibitive for wave function methods such the ones described so far.
The key point about local methods is that a different representation of the wave function is used. Rather than canonical orbitals, which are delocalized over the whole molecular system, localized orbitals (LOs) are employed, whose probability density is concentrated in a limited region of space. In other words we have to apply an unitary transformation to the canonical orbitals:

$$|\vartheta_\iota\rangle = \sum_\nu U_{\nu\iota} \, |\varphi_\nu\rangle \tag{2.34}$$

where $U_{\nu\iota}$ are the elements of an unitary matrix. Using LOs allows us to select only those excitations occurring among orbitals which are close in space. Making considerations based on the chemical sense and on very intuitive distance arguments, this kind of approach achieves surprisingly good results in many cases. This philosophy is not very different from the one adopted by different model Hamiltonians, such as the Hubbard or the Hückel one, which just consider nearest neighbor interactions. However, one main difference has to be kept in mind: while these models employ local Hamiltonians, the local correlation methods use LOs to describe the wave function of a non-local Hamiltonian.
There exist different algorithms which allow us to localize the molecular orbitals according to different criteria, but those employed most for finite systems are the Pipek-Mezey[150] and Foster-Boys[151, 152] localization. The latter, which was employed in this work, minimizes the spatial extent of the LOs by maximizing the distance between their center of charges.
A common issue in the use of localized orbitals is the los of mutual orthogonality when both occupied and virtual orbitals of an HF wave function are localized. This was, for instance, the case for the first applications of localized orbitals in extended systems by Stollhoff and Fulde, who employed a set of non-orthogonal orbitals[53, 153, 154]. This does not prevent us, however, from applying methods such as the particularly successful local second-order Møller-Plesset perturbation theory (LMP2)[62, 63, 155] and local coupled cluster (LCC), whose equations are adapted to the use of non-orthogonal basis. The algorithms employed by these approaches are not very different from the canonical CC and MP2, but, once again, excitations are only allowed into orbitals located in

restricted regions of space. The first applications of these approaches were by Pulay and Saebø, who considered excitations from a set of orthogonal LOs into non-orthogonal projected atomic orbitals (PAOs)[51, 52, 156]. These schemes were extended for the use of other sorts of virtual orbitals, which led to a significant reduction of the number of excitations into the virtual space, *e.g.* pair natural orbitals (PNOs) and orbital specific virtuals (OSVs), as used by Werner and Schütz[157, 158], who also implemented these methods in MOLPRO. Finally, thanks to the work of Pisani and Schütz, LMP2 has also become a state-of-art method for periodic system and is implemented in the CRYSCOR code[63, 155].
Stoll's method of increments (MoI)[64–76] is based on a different scheme, which allows the description of the electron correlation energy as a many-body expansion. The key point of the MoI is that it derives the contributions to the total correlation energy by performing explicit calculations on small fragments of the system, while describing the rest as an environment at the mean-field level. Besides the obvious reduction in scaling, an advantage of the MoI is its flexibility in its application along with any size-extensive quantum-chemical method. Moreover, in its standard formalism, only the occupied orbitals of the HF reference are localized so that mutual orthogonality is not an issue. In this work, we focused in particular on the application of different formalisms of the method of increments which are described in details in section 2.3.1.

2.3.1 The method of increments

As stated, the method of increments aims to describe the correlation energy E_{corr} as a sum of individual contributions (increments) associated with different parts of the system. In order to do so, correlation calculations are performed with a properly defined set of localized orbitals allocated at specific spatial centers, while the rest of the system is kept at the HF level. These groups of LOs are generally referred to as bodies.
Once the bodies into which the system has been split have been chosen, a first crude approximation for the correlation energy can be obtained by the sum of all individual correlation energy contributions associated to each body, the one-body increments ϵ_{i}:

$$E^{(1)}_{\mathrm{corr}} = \sum_{\mathrm{i}}^{\mathrm{N}} \epsilon_{\mathrm{i}} \tag{2.35}$$

At the one-body level, roughly 50-90 % of E_{corr} can be retrieved depending on the choice of the bodies. This is, of course, not enough for chemical precision, but the result can be improved upon step by step by introducing contributions derived from higher order increments. In order to calculate these contributions, one has to consider the correlation between two bodies, three bodies and so on. Therefore, groups of LOs constituting different bodies are included in correlation calculations leading

to values $\epsilon_{\mathrm{ij\ldots z}}$. These finally yield the required increments by subtracting the corresponding lower order increments. As an example, for the two-body increments we have the expression:

$$\Delta\epsilon_{\mathrm{ij}} = \epsilon_{\mathrm{ij}} - (\epsilon_{\mathrm{i}} + \epsilon_{\mathrm{j}}) \tag{2.36}$$

Analogously for the three-body increments we will have:

$$\Delta\epsilon_{\mathrm{ijk}} = \epsilon_{\mathrm{ijk}} - (\Delta\epsilon_{\mathrm{ij}} + \Delta\epsilon_{\mathrm{jk}} + \Delta\epsilon_{\mathrm{ik}}) - (\epsilon_{\mathrm{i}} + \epsilon_{\mathrm{j}} + \epsilon_{\mathrm{k}}) \tag{2.37}$$

Finally, the total correlation energy can be evaluated including all contributions:

$$E_{\mathrm{corr}} = \sum_{\mathrm{i}} \epsilon_{\mathrm{i}} + \sum_{\mathrm{i<j}} \Delta\epsilon_{\mathrm{ij}} + \sum_{\mathrm{i<j<k}} \Delta\epsilon_{\mathrm{ijk}} + \cdots \tag{2.38}$$

Since the electron-electron correlation is short ranged, the increments are expected to decrease as the distance r between the contributing bodies increases. Moreover, since the electronic Hamiltonian is a two-electron operator, it is reasonable to state that high-order increments are expected to be smaller than lower order ones. In formulas we expect that the following conditions are fulfilled:

$$|\Delta\epsilon_{\mathrm{ij}}| > |\Delta\epsilon_{\mathrm{ik}}| \ \text{ for } \ r_{\mathrm{ij}} < r_{\mathrm{ik}} \tag{2.39}$$

$$|\Delta\epsilon_{\mathrm{ij}}| > |\Delta\epsilon_{\mathrm{ijk}}| > |\Delta\epsilon_{\mathrm{ijkl}}| \tag{2.40}$$

If this is the case, the expansion converges rather quickly and a reasonable truncation of the expression in Eq. (2.38) can be done allowing us to successfully apply the method.
The choice of the LOs constituting the bodies is rather arbitrary, as well as the localization pattern employed, but an insight into the electronic structure of the system might help to make a proper partition which allows faster convergence. Moreover, depending on the multireference character of the system, both single-reference and multireference approaches can be used in the MoI framework, by using different sets of LOs. For instance, if CCSD(T) is used, only the occupied orbitals of the HF reference are localized and grouped into bodies, while the virtual orbitals are kept delocalized and used in all correlation calculations. We will refer to such an approach as CCSD(T)-MoI. On the other hand, if a local multiconfigurational character needs to be described, MC-SCF calculations can be performed using bodies which involve both localized occupied and virtual orbitals, allowing the description of the static correlation contributions. In this procedure, which we will refer to as CAS-MoI, only the LOs constituting the chosen body (or bodies) are optimized, while the others are kept frozen. Finally, dynamical correlation can then be calculated by including the remaining delocalized virtual orbitals in a MRCI calculation performed on top of CAS-MoI results. This approached is referred to

as MRCI-MoI.

The MRCI-MoI was shown to be particularly successful in describing situations where static correlations plays an important role, for example for calculating the cohesive energy of bulk alkaline earth metals[70, 159]. Moreover we tested the behavior of this method for the description of the whole dissociation curve a one-dimensional beryllium system, where an avoided crossing has to be observed as described in **Papers M3** and **M4**. Also in this case, the MRCI-MoI yielded very good results, but we were limited by the fact that in different regions of the dissociation curve different HF configurations and therefore different LOs had to be selected. In other words, since the reference used for the localization is not size-consistent, the MoI applied on top of it could not yield size-consistent results. As presented in **Paper M5** and briefly summarized in section 2.3.2, we introduced a formalism that employs a size-consistent CAS-SCF reference for the localization in order to correctly describe the avoided crossing yielding size-consistent results within the MoI framework.

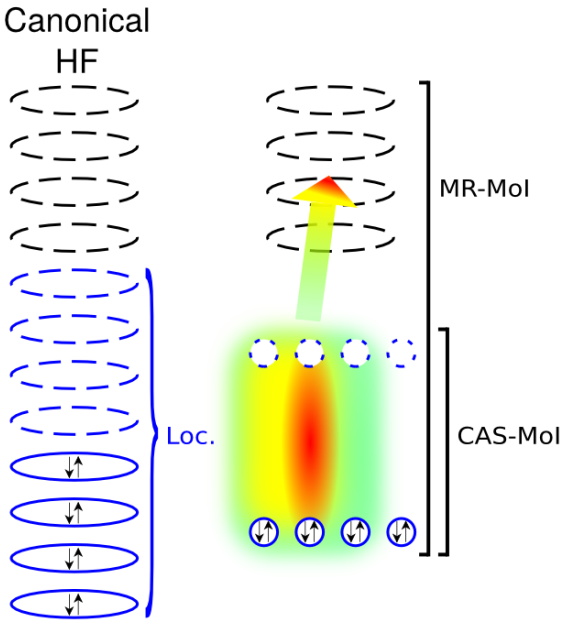

Figure 2.1 Schematic representation of the method of increments (MoI). The ellipses and circles represent canonical and localized orbitals (LOs), respectively. Full lines indicate occupied Hartree-Fock orbitals, while the dash curves represent virtual orbitals. In CAS-MoI the occupied and some of the virtual orbitals are localized and used for the calculation of the increments. In this sketch each body used in CAS-MoI constists of an occupied and a virtual LO. The red, yellow and green areas highligth the groups of orbitals used for one-, two- and three-body calculations. MRCI-MoI calculations are performed on top of the CAS-MoI results by including excitations into the delocalized virtual orbitals as represented by the colored arrow. In the single-reference MoI only occupied HF orbitals are localized and excitations into the delocalized virtual orbitals are performed.

2.3.2 The two-state constant coupling method of increments

In this section we give a brief description of the two-state constant-coupling (TSCC)-MoI, which is presented in more detail in **Paper M5**. In order to address the problem of the lack of size-consistency of the MoI, this approach employs a reference that does not consist of a single configuration, but uses a MC wave function instead. For sake of simplicity, we considered a system which requires two CSFs, $|\phi^{'}\rangle$ and $|\phi^{''}\rangle$, for achieving a size-consistent approximated ground-state wave function $|\tilde{\Phi}_{\mathrm{GS}}\rangle$ in any region of the dissociation curve:

$$|\tilde{\Phi}_{\mathrm{GS}}\rangle = c^{'}_{\mathrm{GS}}\,|\phi^{'}\rangle + c^{''}_{\mathrm{GS}}\,|\phi^{''}\rangle \tag{2.41}$$

By applying two distinct unitary transformations to $|\phi^{'}\rangle$ and $|\phi^{''}\rangle$, two sets of LOs can be obtained and used separately as the basis for MoI calculations, similarly to what was described above. This will yield two sets of increments which can be used to correct the energy of $|\phi^{'}\rangle$ and $|\phi^{''}\rangle$, denoted as $E^{'}$ and $E^{''}$, respectively. Employing a similar expression to Eq. 2.38, one can then calculate the terms:

$$H_{11} = E^{'} + \sum_{\mathrm{i}} \epsilon^{'}_{\mathrm{i}} + \sum_{\mathrm{i<j}} \Delta\epsilon^{'}_{\mathrm{ij}} + \sum_{\mathrm{i<j<k}} \Delta\epsilon^{'}_{\mathrm{ijk}} + \cdots \tag{2.42}$$

$$H_{22} = E^{''} + \sum_{\mathrm{i}} \epsilon^{''}_{\mathrm{i}} + \sum_{\mathrm{i<j}} \Delta\epsilon^{''}_{\mathrm{ij}} + \sum_{\mathrm{i<j<k}} \Delta\epsilon^{''}_{\mathrm{ijk}} + \cdots \tag{2.43}$$

The electron-correlation corrected terms H_{11} and H_{22} do not yield approximations of the energy eigenvalues of the system, but they rather constitute the diagonal elements of a 2×2 Hamiltonian matrix with the corresponding secular equation:

$$\begin{vmatrix} H_{11} - E & H_{12} \\ H_{21} & H_{22} - E \end{vmatrix} = 0 \tag{2.44}$$

The two orthonormal bases implied by Eq. 2.44, $|\phi_1\rangle$ and $|\phi_2\rangle$, correspond to linear combinations of determinants obtained by local excitations from $|\phi^{'}\rangle$ and $|\phi^{''}\rangle$, respectively. However, the calculation of the coupling term $H_{12} = \langle\phi_1|\,\hat{H}\,|\phi_2\rangle$ cannot be achieved via the MoI, since it does not explicitly treat the wave function, but rather deals with corrections to energy only. In order to overcome this problem, one can simply neglect the corrections necessary for describing the full correlated system and use the value $\langle\phi^{'}|\,\hat{H}\,|\phi^{''}\rangle$ instead. As discussed in **Paper M5**, for the chosen system under study, the results are rather satisfactory despite the use of this constant coupling. Moreover, although our main interest is to calculate the ground-state energy in a size-consistent manner, it is remarkable that the solution of Eq. 2.44 yields two energy values, E_{GS} and E_{XS} corresponding to the ground and first excited state, respectively. Although it is not as accurate as E_{GS}, the calculated E_{XS} is in reasonable agreement with a benchmark calculation.

Finally, since each of the two diagonal elements H_{11} and H_{22} requires a single reference ($|\phi^{'}\rangle$ and $|\phi^{''}\rangle$), they can be calculated by applying any MoI formalism discussed so far, including CCSD(T)-, CAS- and MRCI-MoI. According to the method employed in this step we distinguish CCSD(T)-, CAS- and MRCI-TSCC-MoI.

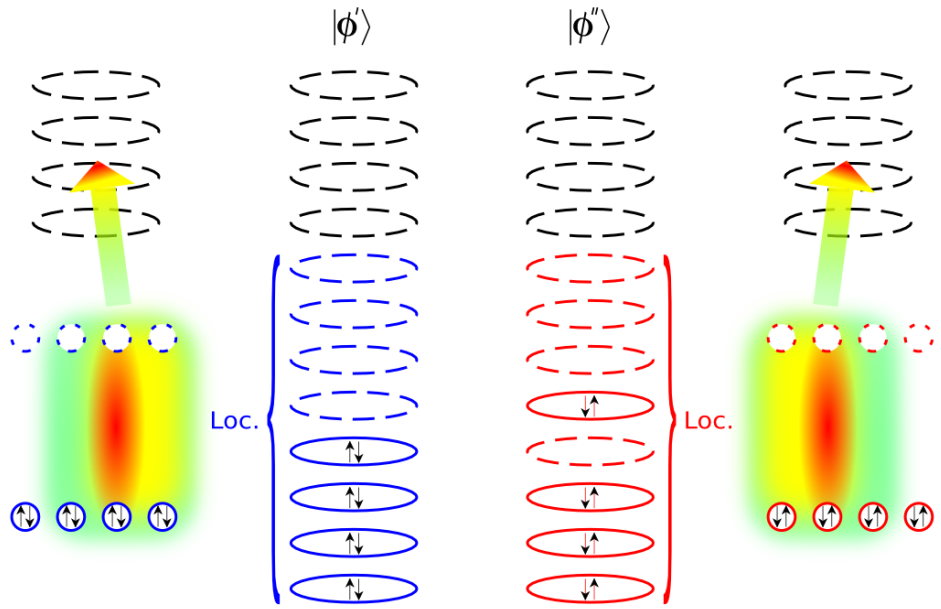

Figure 2.2 In the TSCC-MoI two orbitals of two configurations $|\phi^{'}\rangle$ and $|\phi^{''}\rangle$ are used separately for the incremental calculations. For applying a CAS-TSCC-MoI the occupied and some of the virtual orbitals are localized and used for the calculation of the increments. These are indicate by blue and red curves for $|\phi^{'}\rangle$ and $|\phi^{''}\rangle$, respectively. Full lines indicate occupied orbitals, while the dash curves represent virtual orbitals. The ellipses and circles represent natural and localized orbitals (LOs), respectively. In this sketch each body used in CAS-TSCC-MoI constists of an occupied and a virtual LO. The red, yellow and green areas highligth the groups of orbitals used for one-, two- and three-body calculations. For including the remaing dynamical correlation by means of MRCI-TSCC-MoI, excitations into the delocalized virtual orbitals are included. If CCSD(T)-TSCC-MoI is employed only occupied orbitals are localized and excitations into the delocalized virtual orbitals are performed. Independetly on the level of theory employed, the two energies obtained by the this approach are then used as diagonal elements of a 2×2 Hamiltonian matrix.

2.4 Density matrix renormalization group

In this section we will give a brief overview of the quantum-chemical density matrix renormalization group (QC-DMRG) method as applied in this work and we will depict the machinery of quantum information theory used both by the DMRG algorithm and as a tool for investigating the wave function. The reader interested in more details is referred to the reviews[84–91].

Introduced by Steven R. White in 1992[82, 83], DMRG is a powerful tool for treating quantum many-body systems, in particular for one-dimensional systems. The method is based on the renormalization group (RG) whose first applications in the field of solid state physics dates back to the 1970s, when Kenneth Wilson used it to solve the long-standing Kondo problem[160]. The mathematical machinery of the RG allows us to systematically investigate a physical system by partitioning it into different subsystems and analyzing how the properties under study converge as the subsystem size increases. Original applications of the renormalization group were formulated around truncations of the Hilbert space based on the selection of lowest eigenvalues of subsystem Hamiltonians, but such strategy was not successful for quantum-chemical systems. On the other hand, as we will discuss, DMRG applies a clever machinery, which selects bases according to their importance in the wave function, by analyzing the reduced density matrix.

As described in section 2.2.2, truncated CI methods aim to approximate the FCI wave function by selecting some of the n-electron bases that span the whole Hilbert space $\mathbb{H}$ based on the order of excitation with respect to the HF reference. DMRG aims to truncate the Hilbert space as well, but following a quite different approach based on the approximation of subspaces of $\mathbb{H}$ corresponding to different partitions of the quantum system. Therefore, before introducing DMRG itself, it is first necessary to describe some useful concepts regarding quantum entanglement and its relation to the density matrix, which, as we will see, plays a key role in identifying the most important bases to be considered.

Consider two subsystems A and B with corresponding Hilbert spaces $\mathbb{H}^{(A)}$ and $\mathbb{H}^{(B)}$ spanned by basis functions $|\psi_{\alpha_A}^{(A)}\rangle$ and $|\psi_{\alpha_B}^{(B)}\rangle$ so that $\mathbb{H} = \mathbb{H}^{(A)} \otimes \mathbb{H}^{(B)}$. In these bases the FCI wave function (Eq. 2.4) can be expressed in a state product form as:

$$|\Phi\rangle = \sum_{\alpha_A,\alpha_B} C_{\alpha_A,\alpha_B} |\psi_{\alpha_A}^{(A)}\rangle \otimes |\psi_{\alpha_B}^{(B)}\rangle \tag{2.45}$$

Herein the CI coefficients C_{α_A,α_B} are the elements of the rectangular matrix $\mathbf{C}$ which correspond to a remapping of the coefficient matrix presented in section 2.2.2, where the indices α_A and α_B run over all the possible states that A and B can assume.

By applying a proper unitary transformation, Eq. 2.45 can be rewritten in a much more convenient

form, the Schmidt form:

$$|\Phi\rangle = \sum_{\mathrm{i}}^{r_{\mathrm{sch}}} \sqrt{\omega_{\mathrm{i}}}\, |\zeta_{\mathrm{i}}^{(A)}\rangle \otimes |\zeta_{\mathrm{i}}^{(B)}\rangle \tag{2.46}$$

where the Schmidt bases $|\zeta_i^{(A)}\rangle$ and $|\zeta_i^{(B)}\rangle$ are orthonormal functions which span the Hilbert spaces of A and B. This is clearly a more compact form than Eq. 2.45, not only because only a single sum is involved, but also since the Schmidt rank r_{sch} always obeys the relation $r_{\mathrm{sch}} \leq \min(\dim(\mathbb{H}^{(A)}), \dim(\mathbb{H}^{(B)}))$. The singular values ω_i can be calculated by singular value decomposition (SVD) of $\mathbf{C}$:

$$\mathbf{C} = \mathbf{U}\mathbf{\Omega}\mathbf{V} \tag{2.47}$$

where $\mathbf{U}$ and $\mathbf{V}$ are unitary matrix and the singular matrix $\mathbf{\Omega}$ is a diagonal matrix with elements ω_i (the singular values). It should be noted that it is equivalent to state that the singular values are the eigenvalues of the reduced density matrix (RDM) of subsystem A (or B). Indeed, the RDM of each subsystem contains the complete information regarding the entanglement between the two blocks. It has to be underlined that the size of the Schmidt rank is strongly related to the quantum entanglement of the two subsystems, since only in the case where $r_{\mathrm{sch}} = 1$ can the wave function be exactly factorized in terms of bases of A and B, and the two subsystems are not entangled. It should be clear then, that the Schmidt form becomes more compact as the entanglement between the subsystems reduces. There exist different measures that allow us to quantify the entanglement from the reduced density matrix. The analysis of such quantities constitutes the basics of quantum information theory (QIT)[42, 92–101], which not only allows the study of the physics of a system, but is also essential for improving the performance of DMRG. We will focus on these aspects in subsections 2.4.3 and 2.4.4 after describing the method itself.

It is maybe worthwhile to stress the fact that Eq. 2.46 does not represent any approximation per se. However, it is clear that having access to the reduced density matrix and therefore to its eigenvalues allows us to truncate this expansion by selecting the most important bases which correspond to the largest ω_i. This a key point for understanding the machinery of DMRG and constitutes a strong criterion for the truncation of the Hilbert space.

2.4.1 Two-site DMRG in quantum chemistry

Although there are different formalisms of DMRG, here we will only describe the one applied in this work, which employs the two-site formulation within the finite-lattice method. Consider a system composed of d sites, each of which can show q possible states, so that the dimension of the whole Hilbert space will be q^d. In the realm of quantum chemistry, these sites are spatial orbitals φ_ν with $q = 4$ possible states $|\varphi_{\alpha_\nu}^{(\nu)}\rangle = |-\rangle$, $|\uparrow\rangle$, $|\downarrow\rangle$, or $|\uparrow\downarrow\rangle$. As shown in Fig. 2.3, this d-orbital Hilbert space, arranged in a one-dimensional topology, is decomposed into a left and a right block, composed

respectively of l and $r = d - l - 2$ orbitals and two other orbitals between them. The presence of these two sites is fundamental for truncating the Hilbert space during the DMRG procedure. At each iteration, respectively M_l and M_r of the q^l and q^r bases of the left and right block are chosen. We will refer to these as $|\psi_{\alpha_l}^{(l)}\rangle$ and $|\psi_{\alpha_r}^{(r)}\rangle$, respectively. The $M_l M_r q^2$-dimensional Hamiltonian matrix of the whole system (the superblock) is then constructed in the basis $|\psi_{\alpha_l}^{(l)}\rangle \otimes |\varphi_{\alpha_{l+1}}^{(l+1)}\rangle \otimes |\varphi_{\alpha_{l+2}}^{(l+2)}\rangle \otimes |\psi_{\alpha_r}^{(r)}\rangle$ and diagonalized. This gives one an approximated solution of the FCI problem in a truncated Hilbert space of dimension $M_l M_r q^2 << q^d$. The aim of DMRG is to improve the quality of this solution by selecting the best truncated bases via a series a successive iterations. This is done by diagonalizing the RDM of the subsystem spanned by the bases $|\psi_{\alpha_l}^{(l)}\rangle \otimes |\varphi_{\alpha_{l+1}}^{(l+1)}\rangle$. By applying a SVD, one can then write the wave function in a Schmidt form. Referring to Eq. 2.46, the two subsystems A and B will be constituted by $l+1$ and $r+1$ orbitals, respectively. At this point, one can perform a truncation by selecting $M_l^{\text{kept}} < M_l q$ Schmidt bases corresponding to the largest eigenvalues of the RDM. These new truncated bases have to then be renormalized and will be used in the next iteration.
A new partition of the Hilbert space can then be performed by including a site more into the left block (called system block) and excluding one from the right one (called environment). A new basis can be constructed and the procedure can start again. These iterations will run as described until the environement constists of one site only. When this happens, the roles of system block and environment are switched and the process is repeated in the opposite direction. This procedure is called sweeping. The very first iteration of such procedure will involve a system block with only one orbital, so that the environment involves $d - 3$ orbitals. The choice of the bases of the environment turns out to be crucial not only for speeding up the method, but also for ensuring to be targeting the correct state. The dynamically extended active space (DEAS) procedure allows us to make such choice by selecting some of the $d - 3$ orbitals that will be treated as active in the given DMRG iteration step.

2.4.2 The matrix product state ansatz

The iterative procedure described above requires an ansatz of the wave function which allows us to construct and truncate the Hilbert spaces of different partitions of the system with ease. Tensor networks offer such a powerful mathematical formalism since they allow the decomposition of high order tensors into smaller order ones. Although different forms of the tensor networks exist and can be used as ansatz for the DMRG wave function, in the following we will limit ourselves to the easiest form, the matrix product state (MPS) formalism[90, 91, 102–106]. Let us start by expressing the FCI wave function in a slightly different form:

$$|\Phi\rangle = \sum_{\{\alpha_\nu\}} C_{\alpha_1,\alpha_2,\cdots,\alpha_d} |\varphi_{\alpha_1}^{(1)}, \varphi_{\alpha_2}^{(2)}, \cdots, \varphi_{\alpha_d}^{(d)}\rangle \tag{2.48}$$

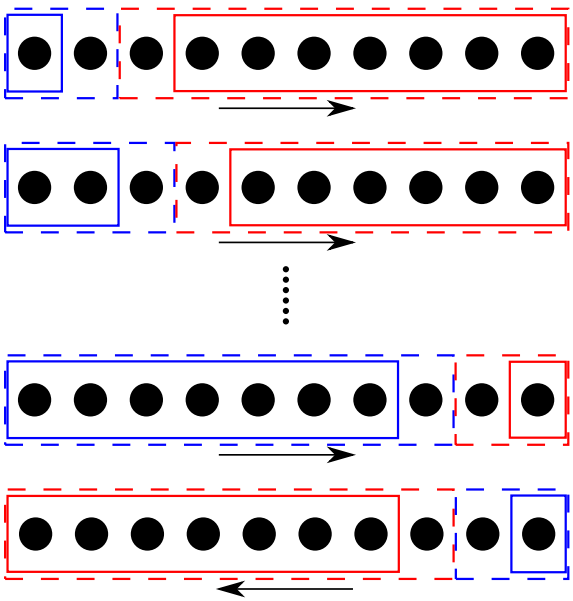

Figure 2.3 Schematic representation of the one-dimensional topology employed in the two-site DMRG in the finite-lattice method. Each dot represents a site or orbital in the quantum-chemical version of DMRG. The system block (of dimension M_l) and the environment (of dimension M_r) are indicated by the blue and red full boxes, respectively.The subsystems indicated by dashed lines have dimension $M_l q$ and $M_r q$. At any iteration, the DMRG procedure select only some of these bases. Then, the system block is enlarged by including one more site. This repeats until the environment consists of one site only. When this happens the sweeping process starts in the opposite direction.

Here the CI coefficients $C_{\alpha_1,\alpha_2,\cdots,\alpha_d}$ are the elements of the FCI tensor $\mathbf{C}$.[2] The indices α_ν run over the four states that each orbital φ_ν can assume, which gives rise to a tensor of order d with a total of 4^d elements. In order to decompose this tensor it is convenient to remap it first into a different form, namely a $4 \times 4^{d-1}$ matrix with elements

$$C_{\alpha_1,\alpha_2,\cdots,\alpha_d} = C_{\alpha_1;(\alpha_2,\cdots,\alpha_d)} \tag{2.49}$$

This allows us to easily apply a singular value decomposition to $\mathbf{C}$:

$$C_{\alpha_1;(\alpha_2,\cdots,\alpha_d)} = \sum_{m_1} U^{(1)}_{\alpha_1,m_1} \Omega^{(1)}_{m_1} V^{(1)}_{m_1;(\alpha_2,\cdots,\alpha_d)} \tag{2.50}$$

$$= \sum_{m_1} A^{(1)}_{\alpha_1,m_1} V^{(1)}_{m_1;(\alpha_2,\cdots,\alpha_d)} \tag{2.51}$$

[2]The tensor $\mathbf{C}$ is equivalent to the coefficient matrix presented in section 2.2.2 with the only difference being that a different remapping is employed.

By repeating a similar operation on $V^{(1)}_{m_1;(\alpha_2,\cdots,\alpha_d)}$ and again on each other emerging matrix, one can finally achieve an expression that decomposes the tensor in terms of d of smaller order:

$$C_{\alpha_1,\alpha_2,\cdots,\alpha_d} = \sum_{m_1}\sum_{m_2}\cdots\sum_{m_{d-1}} A^{(1)}_{\alpha_1,m_1} A^{(2)}_{m_1,\alpha_2,m_2}\cdots A^{(d)}_{m_{d-1},\alpha_d} \tag{2.52}$$

where $A^{(1)}_{\alpha_1,m_1}$ and $A^{(d)}_{m_d,\alpha_d}$ are tensors of order 2, while the remaining $d-2$ $A^{(\nu)}_{m_{\nu-1},\alpha_\nu,m_\nu}$ tensors are of order 3. In Eq. 2.52 the dimension of the bond indices m_ν grows exponentially towards the center of the chain as $\dim(m_\nu) = \min(4^\nu, 4^{d-\nu})$. Therefore, in order to make the MPS ansatz of practical use, a threshold to m_ν has to be employed so that the FCI tensor can be approximated. The selected threshold M is called bond (or virtual) dimension or number of block states and it is a central parameter in DMRG since it determines the accuracy of the results and, as can be proven, the approach is variational with respect to M.

The MPS ansatz is particularly advantageous since it allows us to construct the complete space and subspaces in a hierarchical way. Indeed, one can start defining the bases for the 4-dimensional subspace $\mathbb{H}^{(1)}$ as:

$$|\psi^{(1)}_{m_1}\rangle = \sum_{\alpha_1} A^{(1)}_{\alpha_1,m_1}\,|\varphi^{(1)}_{\alpha_1}\rangle \tag{2.53}$$

From this, one can construct the 16-dimensional tensor product space $\mathbb{H}^{(1,2)} = \mathbb{H}^{(1)} \otimes \mathbb{H}^{(2)}$ which is spanned by the bases:

$$|\psi^{(1,2)}_{m_2}\rangle = \sum_{m_1}\sum_{\alpha_2} A^{(2)}_{m_1,\alpha_2,m_2}\,|\psi^{(1)}_{m_1}\rangle \otimes |\varphi^{(2)}_{\alpha_2}\rangle \tag{2.54}$$

In a similar way one can construct the bases spanning any subspace of $\mathbb{H}$. This is very convenient for the DMRG procedure described in the previous section.

2.4.3 Quantum information theory in DMRG

The orbital ordering in the one-dimensional topology employed in QC-DMRG plays a huge role in the effectiveness of the method. In order to apply this approach as a black box method the analysis of quantum entanglement achievable by the machinery of quantum information theory is applied. As already stated, there are different measurements of the entanglement of quantum subsystems. The one which we employed is the mutual information[93, 161, 162]. Let us start by defining the von Neumann entropy[163]. Given a subsystem A whose reduced density matrix has eigenvalues $\omega^{(A)}_{\mathrm{i}}$, the von Neumann entropy of A is given by:

$$s_A = -\sum_{\mathrm{i}} \omega^{(A)}_{\mathrm{i}} \ln \omega^{(A)}_{\mathrm{i}} \tag{2.55}$$

If A is constituted by a single orbital ν the one-orbital entropy $s(1)_\nu$ can be defined. This quantifies the contribution of an orbital to the total electron correlation. Similarly the two-orbital entropy $s(2)_{\nu\mu}$ can be calculated by considering the two-orbital reduced density matrix. From this, the mutual information can be defined as

$$I_{\nu\mu} = s(2)_{\nu\mu} - s(1)_\nu - s(1)_\mu \tag{2.56}$$

$I_{\nu\mu}$ describes how the two orbitals ν and μ are correlated. This includes both classical correlation and quantum entanglement. In order to improve the effectiveness of DMRG, the MPS should be constructed in such a way that highly entangled orbitals are closer. This way, during the sweeping process the system can be bi-partitioned in such a way as to reduce the Schmidt rank. We introduce the cost function I_{cost} which evaluates the localization of entanglement:

$$I_{\mathrm{cost}} = \sum_{\nu<\mu} I_{\nu\mu}|\nu - \mu|^\eta \tag{2.57}$$

where $|\nu - \mu|$ expresses the distance between the orbitals arranged in the one-dimensional topology. As explained in **Paper M2**, choosing the exponent η equal to 2 allows us to employ the mathematical tools of spectral graph theory[164] according to which the Fiedler ordering[165, 166] minimizes Eq. 2.57. In the same publication we focused on the effect of the one-electron basis on the overall entanglement by comparing the efficiency of DMRG with canonical and localized orbitals. Clearly the basis which allows a reduction of I_{cost} will favour the speeding up of the process.
Also the information provided by $s(1)_\nu$ is employed to speed up DMRG convergence, by allowing the selection of the initial bases of the environment in the first sweeping. This is done by selecting the orbitals with larger one-orbital entropy and using them to construct excited CSFs from the HF CSF. Since it is similar to a CI formalism, the procedure is denoted as CI-DEAS[92, 94].
Another way of improving DMRG performances is the dynamic block state selection (DBSS)[96, 167]. As discussed, DMRG is variational with respect to the number of block states which is kept constant in any cycle in the general formalism. However, depending on the entanglement between the subsystems in a particular cycle of DMRG, the choice of a different M can cause tremendous changes in the performances. The DBSS procedure emploies a different number of block states at every step by fixing a threshold for the quantum information loss χ:

$$\chi = 1 - \sum_{\mathrm{i}} \omega_{\mathrm{i}} \tag{2.58}$$

This quantity measures the error introduced by the truncation of the Hilbert space, since for the FCI wave function $\sum_{\mathrm{i}} \omega_{\mathrm{i}} = 1$.

2.4.4 Entanglement analysis

Although QIT arguments are used as tools to improve the mathematical algorithm in the DMRG procedure, they can also be employed to study the physics of a system. Of course, it is true that they depend on the orbital basis so this information must be examined with care. However, especially in simple one-dimensional systems which can be compared with model Hamiltonians, information about the entanglement of localized orbitals can be connected to the delocalization of the overall wave function. For instance, in **Paper M2** we discussed the dependence of $I_{\nu\mu}$ from the distance between the center of charges of the involved localized orbitals. In fact, for an insulator the orbital entanglement is expected to decay faster than for a metal whose wave function is far more delocalized. Moreover, the information regarding entanglement contained in $I_{\nu\mu}$ can be further analyzed by studying the elements of the two-orbital reduced density matrix[168]. These express the probabilities of the possible transitions $|\varphi^{(\nu)}_{\alpha'_\nu}\rangle \otimes |\varphi^{(\mu)}_{\alpha'_\mu}\rangle \rightarrow |\varphi^{(\nu)}_{\alpha''_\nu}\rangle \otimes |\varphi^{(\mu)}_{\alpha''_\mu}\rangle$. In a localized orbital basis, these transition probabilities can be interpreted as hopping and spin-flipping terms. This distinction of these different contributions is crucial since the study of the decay of the hopping terms with the distance is clearly connected with charge transport. As discussed, the comparison with a physical model, *i.e.* the Hubbard chain, can be used to rationalize such observations.

Finally, the von Neumann entropy of segments of a finite chain (the block von Neumann entropy) can be used to study critical and gapped phases[95, 96, 169]. Indeed, as the block size increases the block entropy is expected to logarithmically diverge for critical systems and to saturate for gapped ones. This connection to the energy spectrum was exploited for investigating metal-insulator transitions.

2.5 The total position-spread tensor

As discussed in the introduction, the Kohn's theory of the insulating state led to the development of the localization tensor (LT) by Souza and Resta[44, 45] as a tool for quantifying the localization of the wave function and therefore the metallic/insulating character. The total position-spread (TPS) tensor $\mathbf{\Lambda}$ introduced by Evangelisti *et al.*[49] is essentially the same as the LT with the difference that $\mathbf{\Lambda}$ is not a value per electron. The name 'spread' rather than 'localization' was chosen since it better reflects the property of this quantity, since larger values of the tensor correspond to a higher delocalization of the wave function.

The TPS tensor shows a size-extensive behavior and its trace is invariant under rotation and translation of the whole molecule. These properties make the TPS tensor an invariant quantity that can be associated to a physical system. By definition, $\mathbf{\Lambda}$ is the second-moment cumulant of the total electron-position operator $\hat{\mathbf{r}} = \sum_{\mathrm{i}} \hat{\mathbf{r}}_{\mathrm{i}}$:

$$\mathbf{\Lambda} = \langle\Phi|\hat{\mathbf{r}}^2|\Phi\rangle - \langle\Phi|\hat{\mathbf{r}}|\Phi\rangle^2 \tag{2.59}$$

From the three cartesian components of $\hat{\mathbf{r}}$, nine elements of $\mathbf{\Lambda}$ originate:

$$\Lambda_{pq} = \langle\Phi|\hat{S}_{pq}|\Phi\rangle - \langle\Phi|\hat{p}|\Phi\rangle\langle\Phi|\hat{q}|\Phi\rangle \quad \text{with} \quad p,q = x,y,z \tag{2.60}$$

The second-moment operator $\hat{S}_{pq}$ is defined as:

$$\hat{S}_{pq} = \sum_{\mathrm{i}}^{n}\sum_{\mathrm{j}}^{n} \hat{p}_{\mathrm{i}}\hat{q}_{\mathrm{j}} \tag{2.61}$$

where the summation indices run over all electrons. It has to be underlined that this two-electron operator is very different from the 'second-moment' operator $\hat{s}_{pq}$[50] defined in codes such as MOLPRO[157] and DALTON[170, 171]:

$$\hat{s}_{pq} = \sum_{\mathrm{i}}^{n} \hat{p}_{\mathrm{i}}\hat{q}_{\mathrm{i}} \tag{2.62}$$

Differently from $\langle\Phi|\,\hat{s}_{pq}\,|\Phi\rangle$, which is an one-electron property, the total position-spread tensor contains information about electron correlation. Indeed, this two-electron property accounts for the position of all pairs of electrons. The diagonal elements of the TPS tensor measure the variance of electron positions, while a non-diagonal element is the covariance of two different components p and q of the total position.

The TPS tensor is a powerful tool for monitoring the electronic wave function for molecular systems

which involve charge transfers[49, 50, 172, 173]. Indeed, by analyzing how its different elements change along a dissociation curve, one can easily investigate bond formations and breakings. For instance, when studying the dissociation of H_2 one observes different behaviors for the longitudinal component of the TPS tensor ($\Lambda_{\parallel}$) in different regions of the dissociation curve. While at dissociation, because of its size-extensive behavior, $\Lambda_{\parallel}$ reaches a plateau, for shorter internuclear distances a maximum appears indicating the maximum delocalization of the wave function. This is interpreted as evidence of the formation of the H-H bond. As the nuclei get closer to each other, the TPS value significantly drops since the effective nuclear charge makes electrons more localized.
As discussed in **Papers m1** and **m2**, the behavior of the TPS tensor at large internuclear distance reflects the presence or absence of charge entanglement in the system. Indeed, while in systems such as H_2 a plateau is reached, molecular systems with large charge delocalizations (for instance H_2^-) will present a divergent behavior of the TPS. This highlights the strong connection between entanglement and localization.
Finally, as already stated, the TPS tensor is a quantity of particular importance in the framework of metal-insulator transitions. Indeed, the cumulant divided by the number of electrons diverges in the thermodynamic limit for a conductor while it converges for an insulator. It is remarkable that, exploiting this rule of thumb, the metallic/insulating behavior of an infinite system can be deduced by studying the TPS tensor of finite chains[172, 174–177].
In the following, we will often refer to the TPS tensor as spin-summed (SS)-TPS tensor to distinguish it from the novel formalism of the spin-partitioned TPS tensor which is introduced in the next section.

2.5.1 The spin partition of the TPS tensor

In this work, besides focusing on the application of the SS-TPS tensor, we developed a new formalism which provides information about the mobility of individual spins, the spin-partitioned (SP)-TPS tensor. Since $\hat{\mathbf{r}}$ can be described as the sum of two terms arising from the α and β electrons, $\hat{\mathbf{r}}_\alpha$ and $\hat{\mathbf{r}}_\beta$, each term in Eq. 2.59 can be split into four contributions:

$$\mathbf{\Lambda} = \mathbf{\Lambda}_{\alpha\alpha} + \mathbf{\Lambda}_{\beta\beta} + \mathbf{\Lambda}_{\alpha\beta} + \mathbf{\Lambda}_{\beta\alpha} \tag{2.63}$$

where the different components of the SS-TPS tensor are:

$$\mathbf{\Lambda}_{\alpha\alpha} = \langle\Phi|\hat{\mathbf{r}}_\alpha^2|\Phi\rangle - \langle\Phi|\hat{\mathbf{r}}_\alpha|\Phi\rangle^2 \tag{2.64}$$

$$\mathbf{\Lambda}_{\beta\beta} = \langle\Phi|\hat{\mathbf{r}}_\beta^2|\Phi\rangle - \langle\Phi|\hat{\mathbf{r}}_\beta|\Phi\rangle^2 \tag{2.65}$$

$$\mathbf{\Lambda}_{\alpha\beta} = \langle\Phi|\hat{\mathbf{r}}_\alpha\hat{\mathbf{r}}_\beta|\Phi\rangle - \langle\Phi|\hat{\mathbf{r}}_\alpha|\Phi\rangle\langle\Phi|\hat{\mathbf{r}}_\beta|\Phi\rangle \tag{2.66}$$

$$\mathbf{\Lambda}_{\beta\alpha} = \langle\Phi|\hat{\mathbf{r}}_\beta\hat{\mathbf{r}}_\alpha|\Phi\rangle - \langle\Phi|\hat{\mathbf{r}}_\beta|\Phi\rangle\langle\Phi|\hat{\mathbf{r}}_\alpha|\Phi\rangle \tag{2.67}$$

Because $\hat{\mathbf{r}}_\alpha$ and $\hat{\mathbf{r}}_\beta$ commute, $\mathbf{\Lambda}_{\alpha\beta}$ and $\mathbf{\Lambda}_{\beta\alpha}$ components are equal, while further symmetry relations occur depending on the system and spin symmetry.

This spin partition is remarkable since it allows us to study how the electron mobility is affected by other same-spin and opposite-spin electrons. In other words, the effects due to Fermi (same spin) and Coulomb correlation (opposite spin) can be separated and analyzed. This provides deeper information about the structure of the wave function and allows the investigation of systems where changes in the electron mobility are related to strong magnetic couplings. Moreover, analogously to the SS-TPS tensor, which gives information concerning charge entanglement, the asymptotic behavior of the SP-TPS is strongly related to the spin entanglement. These properties are briefly explained in Chapter 4 and in details in **Papers m1**, **m2** and **M1** where this formalism was introduced and applied to study hydrogen chains, Hubbard chains and Heisenberg chains.

Chapter 3

Models and computational details

For the realization of this work, different correlation methods were employed with a particular focus on the method of increments (MoI) and the density matrix renormalization group (DMRG). Each step of the MoI procedure was performed within the quantum-chemical package MOLPRO[157], while the DMRG calculations were carried out by employing the QCDMRG-Budapest program package[178] written by the group of Prof. Dr. Örs Legeza. Finally, the calculations of the total position-spread (TPS) tensor and its spin partition were done by means of different programs including MOLPRO, the FCI code NEPTUNUS[179–181] and the code HEISENBERG[182] written by Dr. Muammar El Khatib and myself. Further specifications concerning the computational details of each investigation are reported in the publications presented in Chapter 5. There exhaustive descriptions of the systems under study are also provided. In the present chapter a brief overview of the models employed in this work is provided.

The main focus of this work was the investigation of strongly correlated one-dimensional and pseudo-one-dimensional model systems, that is, chains and rings. Clearly, reducing the dimensionality limits the complexity of the problem, allowing the investigation of relatively large (in one dimension) systems with accurate approaches, which are necessary for correctly describe electron correlation in the thermodynamic limit, *i.e.* infinite chains. Of course, these models do not aspire to represent realistic systems, but they provide rather good test cases for different methods and for studying correlation effects as system size increases and more complexity is introduced into the model.

As described in Chapter 2, in a non-relativistic framework, the most accurate description of a many-electron problem is given by the full electronic Hamiltonian (Eq. 2.3), which in second quantization

is:

$$\hat{\mathcal{H}}_{\mathrm{e}} = \sum_{\substack{\nu,\mu \\ \sigma}} T_{\nu\mu}\hat{c}^{\dagger}_{\nu\sigma}\hat{c}_{\mu\sigma} + \sum_{\substack{\nu,\mu,\tau,\upsilon \\ \sigma,\sigma'}} V_{\nu\mu\tau\upsilon}\hat{c}^{\dagger}_{\nu\sigma'}\hat{c}^{\dagger}_{\mu\sigma}\hat{c}_{\tau\sigma'}\hat{c}_{\upsilon\sigma} \quad \text{with} \quad \begin{cases} T_{\nu\mu} = \langle\varphi_\nu|\,\hat{h}\,|\varphi_\mu\rangle \\ V_{\nu\mu\tau\upsilon} = \langle\varphi_\nu\varphi_\mu|\,\hat{g}\,|\varphi_\tau\varphi_\upsilon\rangle \end{cases} \tag{3.1}$$

Here $\hat{c}^{\dagger}_{\nu\sigma}$ and $\hat{c}_{\nu\sigma}$ are the creation and annihilation operator for the spatial orbitals φ_ν with spin function σ (see Eq. 2.7). $T_{\nu\mu}$ and $V_{\nu\mu\tau\upsilon}$ are one- and two-electron integrals, respectively. Extreme approximations of Eq. 3.1 can be obtained by neglecting specific interactions leading to model Hamiltonians. Although the accuracy of these approaches does not reach the level of quantum-chemical correlation methods, they often provide surprisingly good predictions (considering the level of approximations) about physical phenomena which can be then understood in terms of simple pictures. In particular, the Hubbard Hamiltonian $\hat{\mathcal{H}}_{\mathrm{HUB}}$ is a useful model for describing metal-insulator transitions (MITs)[10, 11, 183, 184]. Here, only hoppings between nearest-neighbor sites are allowed and the Coulomb interaction between electrons occupying the same site are considered. In its most simple form, which describes half-filled single-band linear systems, the Hubbard Hamiltonian is:

$$\hat{\mathcal{H}}_{\mathrm{HUB}} = -t\sum_{\nu=1}^{n-1}\sum_{\sigma}(\hat{c}^{\dagger}_{\nu\sigma}\hat{c}_{\nu+1\sigma} + h.c.) + U\sum_{\substack{\nu,\sigma,\sigma' \\ \sigma\neq\sigma'}} \hat{o}_{\nu\sigma}\hat{o}_{\nu\sigma'} \tag{3.2}$$

Herein, t and U are the next-neighbor hopping integral and the intrasite Coulomb integral, respectively, while $\hat{o}_{\nu\sigma} = \hat{c}^{\dagger}_{\nu\sigma}\hat{c}_{\nu\sigma}$. The importance of the Hubbard Hamiltonian lies in the fact that it allows one to describe MITs simply by tuning the strength of the electron correlation by changing the ratio $-t/U$. Indeed, the equilibrium between the hopping between neighboring sites and the strength of Coulomb electron correlation is the key to determine whether electrons can be prompted to move along the chain and behave as charge carriers. In this work, Hubbard chains were used as test case for the spin-summed (SS)-TPS and the spin-partitioned (SP)-TPS tensor (see section 2.5 **Paper m1**). Also, in **Paper M2** this model Hamiltonian is referred to in order to explain the entanglement analysis obtained for more complex systems in terms of a simple picture.

The limits $-t/U \to \infty$ and $-t/U \to 0$ constitute two particularly interesting situations. In the first case the simple tight-binding Hamiltonian arises, which neglects electron correlation by considering the electron-electron interactions only at a mean-field level. This one-electron model yields qualitatively satisfying results for those systems where the interactions between electrons and the nuclear potential play the major role in determining the metallic/insulating behavior, which can be analyzed in terms of a one-electron band structure. On the other hand, the $-t/U \to 0$ limit of the Hubbard model yields the Heisenberg model[185–187]. Here electrons are fully localized and only interact by magnetic coupling. In its easiest form, which considers a magnetic coupling J_ν equal in any direction,

it becomes:

$$\hat{\mathcal{H}}_{\mathrm{HEI}} = \sum_{\nu=1}^{n-1} J_\nu \left[\frac{1}{2} \left(\hat{\mathbb{S}}_\nu^+ \hat{\mathbb{S}}_{\nu+1}^- + \hat{\mathbb{S}}_\nu^- \hat{\mathbb{S}}_{\nu+1}^+ \right) + \hat{\mathbb{S}}_\nu^z \hat{\mathbb{S}}_{\nu+1}^z \right] \tag{3.3}$$

By allowing different values of J_ν for alternate pairs in the Heisenberg chain, the formation of spin pairs can be studied. This effect can be considered, to some extent, as reflective of the formation of dimers as in the Peierls insulator. These and other aspects of this model are explored in **Paper M1** where it was used as test case for the calculation of the SP-TPS tensor.

It is useful to refer to these models in order to better understand the results of more complex calculations obtained via quantum-chemical methods. For instance, the quantum chemistry 'analog' of a Hubbard chain is a one-dimensional arrangements of hydrogen atoms with only a $1s$ atomic function per hydrogen. This introduces more complexity into the system since it does not only involve next-neighbor interactions. Despite their simplicity, these are good model systems for studying MITs. In the thermodynamic limit, these systems behave as metals in the bound regimes according to an one-electron picture, since they have a half-filled band. On the other hand an insulating behavior occurs by changing the distance between the hydrogen atoms: Peierl insulators occur if dimers form which force the electronic band to split into a valence fully occupied band and a virtual empty band, while at dissociation the system behaves as an insulator since hoppings from one site (atom) to another cannot be promoted. Once again, simplified pictures of such a system can be understood in term of a model Hamiltonian. In **Papers m1** and **m2** the SS-TPS and SP-TPS tensor of these systems were calculated and discussed.

More and more complexity can be added to the models by adding more electronic bands, that is, by using larger one-electron basis sets and/or by employing an analogous system consisting of lithium atoms, where the excitations into the low-lying $2p$ bands play an important role in the electronic structure (see **Paper M2**). However, static correlation becomes much more important for the description of beryllium, which is given particular attention in this work. Beryllium systems show some interesting features which made them good candidate for test studies. Formally described by the configuration $[\mathrm{He}]2s^2$, the electronic ground state of beryllium atom ^1S_g presents a high static correlation which constitutes the 93 % of its total correlation energy and can be described by excitations into the $2p$-orbitals. Static correlation plays a major role in the description of Be clusters as well. For instance, the bond of the dimer cannot be described properly if a multireference approach is not employed[188–193]. As described more in details in **Paper M4**, this is true also for larger systems.

Beryllium is also particularly interesting in the framework of electrical conductivity since according to a one-electron picture it should be expected to be an insulator with a full valence $2s$ band. Clearly, the near degeneracy of the $2s$ and $2p$ shells play a key role in the metallic/insulating character of this material. Moreover, the role of dimensionality is also of particular interest. Indeed, while bulk

beryllium is clearly a conductor, this is not necessarily the case for one-dimensional beryllium chains. The complexity of this behavior and yet the simplicity of the system make it a perfect subject for low-time-consuming tests.

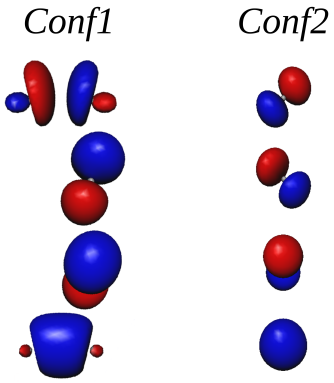

Figure 3.1 Representation of the valence localized orbitals (LOs) of the Be_6 ring as obtained by two main HF configurations, $2a_{1g}^2 2e_{1u}^4 2e_{2g}^4 1b_{2u}^2$ ($Conf1$) and $2a_{1g}^2 2e_{1u}^4 2e_{2g}^4 2b_{1u}^2$ ($Conf2$). For each Be atom four orbitals are obtained, one of which is doubly occupied at the HF level, while the others are virtual orbitals. In different regions of the dissociation curve, one of the two configurations is dominant and the corresponding set of LOs is employed by the standard method of increments.

In order to exploit symmetry at its best, ring structures can be treated rather then linear chains. This allows a significant reduction of the number of calculations required when using the MoI and to avoid border effects which can cause problems in the localization procedure. Moreover, the use of cyclic systems allows one to artificially reproduce the Born von Karman boundary conditions[24] and connect the results obtained for finite systems to the limit corresponding to a periodic chain. **Papers M2-5** are dedicated to the investigation of beryllium rings.

In order to describe the whole dissociation of such Be rings in their ground state $^1A_{1g}$, two main configurations have to be considered. This is shown by the analysis of the CI vectors presented in **Paper M4** and by the occupation patterns reported in **Paper M5**. At dissociation, the n atoms with main configuration $1s^2 2s^2$ give rise to the HF wave function with valence configuration $2a_{1g}^2 2e_{1u}^4 2e_{2g}^4 2e_{3u}^4 \ldots 2b_{1u}^2$ (labeled as $Conf2$) according to the IRREPs of the point group $\mathcal{D}_{nh}$. However, as the distance decreases, the LUMO, which has a pure p character ($1b_{2u}$), approaches the HOMO ($2b_{1u}$) until a crossing between these two orbitals occurs. Here an avoided crossing between two $^1A_{1g}$ states is expected and in the short internuclear distance regime the ground configuration becomes $2a_{1g}^2 2e_{1u}^4 2e_{2g}^4 2e_{3u}^4 \ldots 1b_{2u}^2$ ($Conf1$). As a consequence, a size-consistent (see section 2.2.5) result cannot be achieved via HF and at least a CAS(2,2) which involves $Conf1$ and $Conf2$ has to be used instead. Moreover in order to ensure size-extensivity and give a meaningful description of the dissociation, a reference CAS($2n$, $4n$) is necessary. Since this becomes prohibitive as system size grows, the MoI was applied to treat

large systems (see **Papers M3-5**). Because $Conf1$ and $Conf2$ are predominant in different regions of the dissociation curve and they give rise to very different localized orbitals (see Fig. 3.1), both had to be employed in the MoI. As described in Chapter 4, in order to ensure size-consistency a reference consisting of both configurations was employed and tested in the two-state constant-coupling (TSCC)-MoI formalism to which section 2.3.2 and **Paper M5** are dedicated.

Chapter 4

Results

This chapter briefly summarizes the results presented in the scientific publications produced during the preparation of this thesis. For a more detailed description the reader is referred to **Papers m1-2** and **M1-5**, which are collected in Chapter 5. In section 4.1 some preliminary results which have not yet been published are also presented.

Let us start by describing the publications regarding the analysis of the total position-spread (TPS) tensor and its spin partition, **Papers m1** and **m2**, and **M1** which were produced in collaboration with the groups of Prof. Dr. Stefano Evangelisti and Prof. Dr. Thierry Leininger. As described in section 2.5, the spin-summed (SS)-TPS tensor allows us to describe the localization of the wave function by achieving information about the mobility of electrons in molecules and extended systems. As described, this is important for understanding phenomena that involve charge transfer. Moreover, in the framework of the MIT, the analysis of the convergence/divergence of the SS-TPS as the system size grows towards the thermodynamic limit, allows us to distinguish between an insulating and a metallic state. The power of the this formalism can be further enhanced by splitting the total electronic position operator according to spin variables as described in section 2.5.1 and in details in **Paper m1**, where the formalism of the spin-partitioned (SP)-TPS tensor was first introduced. While the SS-TPS gives information about charge mobility, the SP-TPS tensor is related to spin fluctuations.

We first focused on the simple case of hydrogen molecule and ions in different electronic states, and demonstrated that the behavior of the tensor at large internuclear distances is strongly related to the presence or absence of entanglement. In particular, we observed that for those states characterized by a distinct charge entanglement, the SS-TPS tensor diverges towards dissociation. In a similar way spin-entangled states present a diverging SP-TPS tensor.

Equally spaced hydrogen chains (up to H_{16}) were also investigated and the results were compared with the ones obtained for a Hubbard Hamiltonian. As expected, the analysis of the SS-TPS for the latter shows that the charge mobility increases as the ratio $-t/U$ goes to infinity, which corresponds to

the non-correlated limit (see Chapter 3). The metallic behavior in this regime, reflected by a vanishing energy gap in the thermodynamic limit, is highlighted by the linear growth of the normalized SS-TPS as a function of system size. Similarly, the SS-TPS of hydrogen chains presents a maximum corresponding to a high charge mobility, whose value diverges as the number of H atoms increases. On the other hand, for shorter internuclear distances and towards dissociation the normalized SS-TPS tensor converges with the number of atoms. This change in the trend of the SS-TPS as a function of system size in different regions of the dissociation curve is an evidence of a transition between an insulating and a metallic character as the interatomic distance decreases.

The SP-TPS of an hydrogen chain shows a very different behavior. In fact, it presents a quadratical growth at long distances, which once again is related to a large spin mobility in these strongly entangled systems. To confirm these relations, in **Paper m2** the SP-TPS formalism was also applied to dimerized hydrogen chains, which represent a model for Peierls insulators. As expected, the formation of spin pairs as a consequence of dimerization causes the SP-TPS to drop with respect to the equally spaced chains. In **Paper M1** a further study of the behavior of the SP-TPS was performed by focusing on another model Hamiltonian which explicitly describes spin interaction, the Heisenberg Hamiltonian. By varying the coupling between neighboring spins in order to describe spin pairing and by focusing on different spin states, we analyzed some interesting behaviors. In particular both the ferromagnetic (high-spin) and the anti-ferromagnetic (low-spin) state were studied. By increasing the number of sites, a clear relation between the energy-gap closure-rate and the divergence of the SP-TPS was observed, which is remarkably reminiscent of the trend observed for the SS-TPS, which diverges for gapless systems. Moreover, by performing a full diagonalization of the Heisenberg Hamiltonian we were able to gain information about the SP-TPS for the whole energy spectrum. Although neither the ferromagnetic nor the antiferromagnetic state constitute a lower or an upper bound to the the SP-TPS, it is interesting to note how the average value increases with the energy, indicating an increase of the spin delocalization in the wave function. Also, for the high-spin case we derived an analytical expression of the dependence of the SP-TPS on the number of sites and on the z-projection of the total spin.

For the low-spin case, the use of alternating magnetic couplings allowed us to investigate the effect of spin pairing. This demonstrated analogous results to what was observed for dimerized hydrogen chains, where a lower spin-delocalization occurs as the spin pairing increases. Also in this case a strong relation to the energy gap could be observed.

Although the analysis of SS-TPS and SP-TPS for hydrogen chains and model Hamiltonians led to interesting observations and highlighted the kind of informations that it embodies, in order to make predictions on realistic systems we need to apply the formalism to more complex situations as done by Bendazzoli *et al.*[174–177] at the CAS-SCF and FCI level of theory. However, since these sophisticated descriptions of the wave function are unfeasible for extended systems, different

approaches have to be applied. As described in Chapter 3, our model systems consisting of beryllium rings require an accurate description of static and dynamical correlation effects. Our goal was to correctly describe the dissociation curves of such systems by means of the method of increments (MoI). We focused on this approach in particular because of its favorable scaling that allows the calculation of the correlation energy for very large systems and can be succesfully applied to periodic systems as well. For this reason the MoI is a perfect candidate for approaching the thermodynamic limit. We focused on the application of the MoI and on the difficulties arising by its application for describing a dissociation curve in **Papers M3-5**.

However, as a first step we applied another sophisticated method with favorable scaling to obtain useful benchmarks for the MoI, the density matrix renormalization group (DMRG), which is briefly described in section 2.4. The DMRG results obtained for both beryllium and lithium in collaboration with Prof. Dr. Örs Legeza's group are presented in **Paper M2**. There, besides obtaining a full dissociation curve for Be rings, we focused on different aspects of both the calculation procedure and the entanglement analysis which can be achieved by the use of quantum information theory (QIT) and used to better understand metal-insulator transitions. As stated in section 2.4.4, by analyzing the orbital entanglement the changes occurring in the wave function between a metallic-like state and an insulating state can be investigated. This was done by studying the von Neumann entropy and the elements of the two-orbital reduced density matrix in a localized orbital basis. In this analysis the main distinction between the two states lies in the different decays of the entanglement with distance. This is particularly straightforward for the lithium rings, whose behavior is particularly reminiscent of the half-filled Hubbard Hamiltonian and shows the expected decay of the hopping matrix elements. Also the block von neumann was employed as index for MITs. Indeed, by studying its dependence on the block size we could estimate whether the system evolves towards a gapless or gapped situation. In the case of Be rings the situation is complicated by multiband effects, but also here the entanglement analysis shows an evident change in the structure of the wave function in different regions of the dissociation curve as well.

Finally, we took on the challenge offered by the system as a chance to study the role played by the orbital basis onto the performance of the code. By comparing canonical orbitals with localized orbitals (LOs), we showed that the latter performed much better than the canonical one-electron bases since LOs lead to a strong reduction of the orbital entanglement which has a crucial effect in quantum-chemical DMRG.

The DMRG results obtained for Be rings of different sizes were used as precious benchmarks for testing the method of increments in **Paper M3**. The CAS-MoI formalism (see section 2.3.1) was first applied using a minimal basis set. Although this did not provide an accurate description of the system, it was a valuable case study for testing whether the method is reliable for the calculation of a whole dissociation curve. The CAS-MoI allows us to describe the dissociation curve, but it has limitations

where an avoided crossing occurs. Indeed, this approach is based on localized one-electron functions obtained by a single configuration. Since for this system in different regions of the dissociation curve two different HF configurations are dominant, a choice had to be made, which led to discontinuities in the dissociation curve. In other words, the approach is not fully size-consistent (see section 2.2.5). Nevertheless, since the MoI looses accuracy only at the crossing, as was shown by the comparison with DMRG results, we could use it to investigate the size dependence of the correlation energy in order to extrapolate the values for the periodic chain. These results encouraged us to use the same procedure in order to achieve a better description of the system by using better basis sets and including dynamical correlation through MRCI-MoI calculations on top of CAS-MoI results, as detailed described in **Paper M4**. By doing so, we underlined to importance of accurate size-extensive corrections. Indeed, if these are not correctly described the high-order increments accumulate a substantial error which diverges as system size increases. Finally, by describing the evolution of the electronic structure of beryllium chains and rings, which gained an overview of the system from the dimer to the infinite chain.

Finally, we addressed the problem of the lack of full size-consistency in **Paper M5** where we introduced the two-state constant-coupling (TSCC)-MoI. As described in section 2.3.2 the approach employs the MoI formalism in order to calculate diagonal matrix elements of a 2×2 Hamiltonian matrix constructed by starting from the two main configurations. In the TSCC-MoI the off-diagonal elements are simply approximated by using the results of a SA-CAS-SCF calculations. We applied this procedure to Be rings of different sizes by employing different methods to calculate the diagonal elements via the MoI formalism. DMRG was once again used as a benchmark for testing the validity of the approximation and showed a very good agreement for the ground state.

Once that we were able to achieve accurate results via the MoI formalism for Be rings, we decided to apply the method to calculate other properties besides the energy, in particular the SS-TPS. Analogous equations to the ones used to expand the correlation energy can be used for calculating other properties as shown in the following section, where we also report the preliminary data obtained in such a way for the TPS tensor of the Be_6 ring.

4.1 Calculation of the SS-TPS via the method of increments

As discussed, the MoI allows us to express the correlation energy as a many-body expansion (see section 2.3.1). In principle, very similar equations can be applied to the calculations of other properties which are not scalars as the energy[80, 81]. In this section, we discuss how this can be done to calculating tensorial properties like the SS-TPS tensor, $\mathbf{\Lambda}$. Let us consider a system for which a single HF configuration, with associated TPS tensor $\mathbf{\Lambda}_{\mathrm{HF}}$, is a good first approximation of the wave function and the MoI expansion. Just as we can associate to the i^{th} body a contribution ϵ_{i} to E_{corr}, we can also calculate a contribution $\boldsymbol{L}_{\mathrm{i}}$ to $\mathbf{\Lambda} - \mathbf{\Lambda}_{\mathrm{HF}}$:

$$\boldsymbol{L}_{\mathrm{i}} = \mathbf{\Lambda}_{\mathrm{i}} - \mathbf{\Lambda}^{\mathrm{HF}} \tag{4.1}$$

where $\mathbf{\Lambda}_{\mathrm{i}}$ is calculated by correlating the electrons of the i^{th} body only. Once again this is analogous to the definition of ϵ_{i} and similarly to Eq. 2.35, one 1-body level approximation of the TPS as:

$$\mathbf{\Lambda}^{(1)} = \sum_{\mathrm{i}}^{N} \boldsymbol{L}_{\mathrm{i}} + \mathbf{\Lambda}^{\mathrm{HF}} \tag{4.2}$$

Moreover, in a similar way to what expressed in Eqs. 2.36 and 2.37 for the correlation energy, one can define tensorial 2-body and 3-body increments as:

$$\Delta\boldsymbol{L}_{\mathrm{ij}} = \mathbf{\Lambda}_{\mathrm{ij}} - \mathbf{\Lambda}_{\mathrm{HF}} - \boldsymbol{L}_{\mathrm{i}} - \boldsymbol{L}_{\mathrm{j}} \tag{4.3}$$

$$\Delta\boldsymbol{L}_{\mathrm{ijk}} = \mathbf{\Lambda}_{\mathrm{ijk}} - \mathbf{\Lambda}_{\mathrm{HF}} - \Delta\boldsymbol{L}_{\mathrm{ij}} - \Delta\boldsymbol{L}_{\mathrm{ik}} - \Delta\boldsymbol{L}_{\mathrm{jk}} - \boldsymbol{L}_{\mathrm{i}} - \boldsymbol{L}_{\mathrm{j}} - \boldsymbol{L}_{\mathrm{k}} \tag{4.4}$$

By summing up all the contributions one can finally calculate the TPS for the whole system. The main difference with respect to the application of the MoI for the calculation of scalar properties arises from the fact that the tensors $\boldsymbol{L}_{\mathrm{i}}$ are not equal if the corresponding bodies are symmetry equivalent, which is the case for ϵ_{i}. Nevertheless, point group theory allows us to relate these tensors with each other by applying unitary transformations involving the symmetry operations of the group. For instance if the j^{th} and i^{th} body are connected by the operation represented by the matrix $\boldsymbol{R}$, one can write:

$$\boldsymbol{L}_{\mathrm{j}} = \boldsymbol{R}^{T}\boldsymbol{L}_{\mathrm{i}}\boldsymbol{R} \tag{4.5}$$

Let us consider the special case where all bodies are related by symmetry operations. This is for example the case of the ring structures under study where the bodies are clearly related by rotations, as well as periodic chains, in which translations have to be considered instead. In this situation the

sum occurring in Eq. 4.1 can be rewritten as:

$$\sum_{\mathrm{i}}^{N} \mathbf{L}_{\mathrm{i}} = \sum_{R} \boldsymbol{R}^{T} \boldsymbol{L}_{\mathrm{i}} \boldsymbol{R} \tag{4.6}$$

This helps reduce the amount of calculations that have to be performed, as a single 1-body increment has to be calculated. Analogous equations can be written also for higher order increments.
We performed some preliminary calculations on the Be_6 ring with a minimal $[9s, 4p] \rightarrow (2s, 1p)$ basis set in order to test this approach. In Fig. 4.1 the data for internuclear distances 2.10 Å and 3.00 Å are reported. These particular structures were chosen because they are representative of the two regimes of the dissociation curve. As was done in **Papers M3** and **M4** the two configurations $Conf1$ and $Conf2$ were used for the localization in the two regimes and CAS-MoI was applied. As one can see, as more and more increments are included, both the xx and zz components of the TPS tensor unequivocally converge towards a value very close to the one obtained via RAS(4,24). Unfortunately the convergence is not monotonic and, especially for 2.10 Å, the two body contribution strongly overestimates the contribution given by electron correlation. Nevertheless, considering how much the HF values deviate from the correlated ones, it is very promising that the data obtained via the CAS-MoI deviate with respect to the RAS data by 4 % in the long distance regime and less than 1 % in the short distance regime.

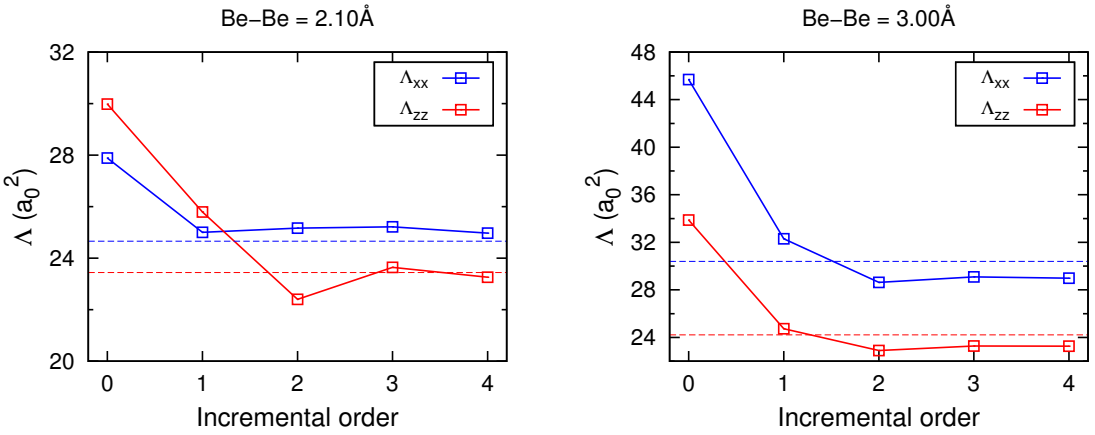

Figure 4.1 Total position-spread (TPS) tensor of the Be_6 ring calculated for two different internuclear distances (2.10 Å and 3.00 Å) with the method of increments employing a minimal $[9s, 4p] \rightarrow (2s, 1p)$ basis set. Both Λ_{xx} and Λ_{zz} components of the TPS tensor are reported as a function the incremental order and compared with the values achieved via a RAS(4,24).

Since we are mostly interested in the crossing region of the dissociation curve, a slightly different approach based on the TSCC-MoI was applied. Once again the mathematics is very similar to what

done for the energy with a few differences. As in section 2.3.2 consider a ground-state wave function which requires a linear combination of two determinants for a size-consistent description (Eq. 2.41). After applying the TSCC-MoI one can calculate the expansion coefficients of the bases implied by Eq. 2.44, c_1^{GS} and c_2^{GS}:

$$|\Phi_{\mathrm{GS}}\rangle = c_1^{\mathrm{GS}} |\phi_1\rangle + c_2^{\mathrm{GS}} |\phi_2\rangle \tag{4.7}$$

This allows us in principle to evaluate other expectation values of $|\Phi_{\mathrm{GS}}\rangle$. In the case of the TPS tensor, we can write:

$$\boldsymbol{\Lambda_{GS}} = c_1^{\mathrm{GS}^2} \boldsymbol{\Lambda_{11}} + c_2^{\mathrm{GS}^2} \boldsymbol{\Lambda_{22}} + 2 c_1^{\mathrm{GS}} c_2^{\mathrm{GS}} \boldsymbol{\Lambda_{12}} \tag{4.8}$$

where $\boldsymbol{\Lambda_{11}}$ and $\boldsymbol{\Lambda_{22}}$ are calculated as described above:

$$\boldsymbol{\Lambda_{11}} = \boldsymbol{\Lambda}^{'} + \sum_{\mathrm{i}} \boldsymbol{L}_{\mathrm{i}}^{'} + \sum_{\mathrm{i<j}} \Delta \boldsymbol{L}_{\mathrm{ij}}^{'} + \sum_{\mathrm{i<j<k}} \Delta \boldsymbol{L}_{\mathrm{ijk}}^{'} + \cdots \tag{4.9}$$

$$\boldsymbol{\Lambda_{22}} = \boldsymbol{\Lambda}^{''} + \sum_{\mathrm{i}} \boldsymbol{L}_{\mathrm{i}}^{''} + \sum_{\mathrm{i<j}} \Delta \boldsymbol{L}_{\mathrm{ij}}^{''} + \sum_{\mathrm{i<j<k}} \Delta \boldsymbol{L}_{\mathrm{ijk}}^{''} + \cdots \tag{4.10}$$

Here $\boldsymbol{\Lambda}^{'}$ and $\boldsymbol{\Lambda}^{''}$ are the TPS tensors for the references $|\phi^{'}\rangle$ and $|\phi^{''}\rangle$, respectively. Each of these determinants is localized and two different sets of increments are calculated as was done for the energy in section 2.3.2. Following the same approximation that we used for the energy, the term $\boldsymbol{\Lambda_{12}} = \langle\phi_1| \hat{\mathbf{r}}^2 |\phi_2\rangle$ can be approximated as $\langle\phi^{'}| \hat{\mathbf{r}}^2 |\phi^{''}\rangle$. However this is zero in the case under study. The absence of a value for the coupling is unfortunate and will have strong repercussions on the accuracy of the results.

Nevertheless, we used this approach to calculate the change in the TPS around the crossing region. For the sake of testing a minimal basis set was used and in absence of a definitive benchmark, different RAS-SCF results were used for comparison. Such data and the ones obtained via TSCC-CAS-MoI at the 3-body level are reported in Fig. 4.2. As one can see, as the description of electron correlation improves, the TPS drops and an evident shift in the position of the crossing occurs, which corresponds to the position of the maximum of the TPS. In general the MoI results follow the correct trend both of TPS value and maximum position. However, these results are still preliminary and further investigation to evaluate a coupling term within the MoI approach are necessary before moving on to the calculation of the TPS for larger rings in order to estimate its behavior in the thermodynamic limit. Nevertheless, these results are promising and the chance of calculating such an interesting quantity via a local approach warrants further study.

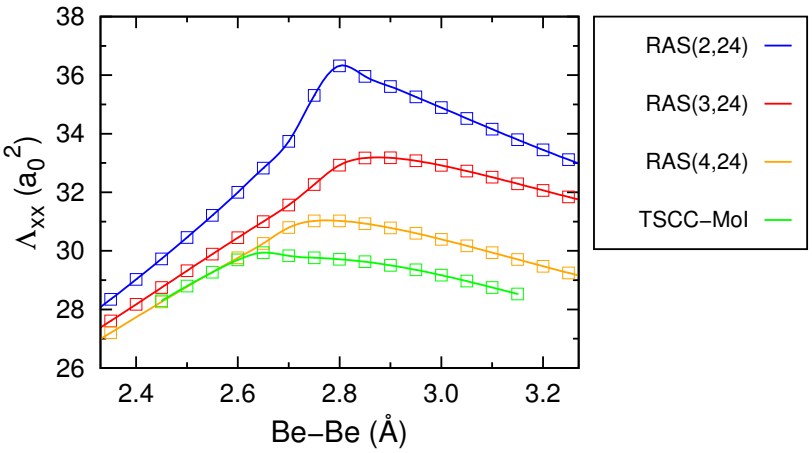

Figure 4.2 Λ_{xx} component of the TPS tensor of the Be_6 ring calculated with the TSCC-CAS-MoI approach at the three-body level in comparison to different RAS-SCF calculations. A minimal $[9s, 4p] \rightarrow (2s, 1p)$ basis set was employed.

Chapter 5

Publications

In this chapter the scientific publications composing this dissertation are presented. These works are divided into two groups according to the importance of my contribution, *i.e.* minor (**m**) or major (**M**). For **Paper m1** and **m2**, I was mainly involved in the interpretation of the data and I partially contributed to the writing of the publications. My contribution to the production of **Paper M1-5** was much larger: I personally produced most of the data reported therein, together with Dr. Muammar El Khatib (**Paper M1**), Dr. Gergely Barcza (**Papers M2**, **M3** and **M5**) and Daniel Koch (**Papers M4** and **M5**). Moreover, I did most of the data analysis and of the writing of these papers.

5.1 Paper m1

"The total position-spread tensor: spin partition"

M. El Khatib, O. Brea, E. Fertitta, G. L. Bendazzoli, S. Evangelisti, T. Leininger

J. Chem. Phys. **142**, 094113 (2015)
DOI 10.1063/1.4913734
URL http://dx.doi.org/10.1063/1.4913734

5.2 Paper m2

"Spin delocalization in hydrogen chains described with the spin-partitioned total position-spread tensor"

M. El Khatib, O. Brea, E. Fertitta, G. L. Bendazzoli, S. Evangelisti, T. Leininger, B. Paulus

Theor. Chem. Acc. **134**, 29 (2015)
DOI 10.1007/s00214-015-1625-7
URL http://dx.doi.org/10.1007/s00214-015-1625-7

5.3 Paper M1

"The spin-partitioned total position-spread tensor: An application to Heisenberg spin chains"

E. Fertitta, M. El Khatib, G. L. Bendazzoli, S. Evangelisti, T. Leininger, B. Paulus

J. Chem. Phys. **143**, 244308 (2015)
DOI 10.1063/1.4936585
URL http://dx.doi.org/10.1063/1.4936585

5.4 Paper M2

"Investigation of metal-insulator-like transition through the *ab-initio* density matrix renormalization group approach"

E. Fertitta, B. Paulus, G. Barcza, Ö. Legeza

Phys. Rev. B **90**, 245129 (2014)
DOI 10.1103/PhysRevB.90.245129
URL http://dx.doi.org/10.1103/PhysRevB.90.245129

5.5 Paper M3

"On the calculation of complete dissociation curves of closed-shell pseudo-one-dimensional systems via the complete active space method of increments"

E. Fertitta, B. Paulus, G. Barcza, Ö. Legeza

J. Chem. Phys. **143**, 114108 (2015)
DOI 10.1063/1.4930861
URL http://dx.doi.org/10.1063/1.4930861

5.6 Paper M4

"Calculation of the static and dynamical correlation energy of pseudo-one-dimensional beryllium systems via a many-body expansion"

D. Koch, E. Fertitta, B. Paulus

J. Chem. Phys. **145**, 024104 (2016)
DOI 10.1063/1.4955317
URL http://dx.doi.org/10.1063/1.4955317

5.7 Paper M5

"Towards a fully size-consistent method of increments"

E. Fertitta, D. Koch, B. Paulus, G. Barcza, Ö. Legeza

arXiv:1605.03904 [physics.chem-ph]
Submitted to *J. Comp. Theor. Chem.* in May 2016
URL http://arxiv.org/abs/1605.03904

Chapter 6

Conclusions and outlook

An *ab-initio* description of the conducting properties of an electronic quantum system requires an accurate treatment of electron correlation. Indeed, the electron-electron Coulomb repulsion plays a key role in determining whether electrons behave as free carriers or whether they are strongly localized. The connection between a vanishing electrical conductivity and the many-body localization of the electronic wave function was highlighted by Kohn in his seminal work of 1964[37] and is reflected by the findings of Nevill Mott[9, 30–33], regarding the nature of the insulating state. Achieving an insight into the many-body wave function is crucial in order to characterize the metallic and insulating behavior. This requires a quantitative measure of the electron mobility and of the quantum entanglement, which are strongly connected concepts. In this work different tools which allow such investigations were presented. As test cases, one-dimensional systems were selected, which consist of both model Hamiltonians (i.e. Hubbard's and Heisenberg's) and linear and ring-shaped monoatomic clusters described by means of quantum-chemical methods.

The total position-spread (TPS) tensor constitutes a powerful formalism to study the electron mobility and it yields an indirect measure of electron correlation. Since a larger value of the TPS tensor corresponds to a larger delocalization of the wave function, this formalism is particularly useful for investigating charge transfers in molecular and extended systems and it is strongly connected to the theory of conductivity. Indeed, a key property of the TPS tensor in the framework of metal-insulator transitions (MITs) is that it diverges for metals while it converges for insulators as system size increases towards the thermodynamic limit[44, 45, 174–177]. In this work we analyzed this behavior for one-dimensional model systems, starting from Hubbard chains (see **Paper m1**), which constitute the simplest model for studying MITs[10, 11, 183]. As electron correlation is gradually switched off by increasing the ratio $-t/U$, the electron mobility increases reaching a maximum in the uncorrelated limit ($-t/U \to \infty$). By studying the behavior of the TPS tensor as a function of chain length, the divergence predicted for a metallic character is observed. A similar behavior was observed

for hydrogen chains described by quantum-chemical methods. Once again, as system size increases, the TPS tensor diverges, which is a symptom of a metallic character. This occurs, however, only in a restricted region of the dissociation curve, while at dissociation and for very short internuclear distances the TPS tensor reveals a reduced electron mobility. This indicates that these are insulating regimes.

As stated, the TPS tensor provides information about entanglement. This connection was highlighted by studying the behavior of the TPS tensor in the long interatomic-distance regime. For instance, the TPS tensors of the H_2 molecule and ions (H_2^+ and H_2^-) were studied for different states. A divergent behavior for long interatomic distances was observed for those states where the electron mobility increases because of charge entanglement (see **Paper m2**).

In this work, a new formalism of the TPS tensor was developed and applied. By means of the novel spin-partitioned (SP)-TPS tensor, the mobility of individual spins can be analyzed. In particular, we defined its equal-spin and different-spin components and studied their behavior for hydrogen chains, Hubbard chains and Heisenberg spin chains (see **Paper M1**). As discussed, this tool is particularly useful for investigating those systems where large spin fluctuations occurs. This deeper insight into the electronic wave function allows the analysis of spin transfers and spin entanglement. This is analogous to the role played by the spin-summed (SS)-TPS tensor for the study of charge transfers and charge entanglement. Moreover, the partition into equal-spin and opposite-spin components offers the chance to distinguish pure Coulomb-correlation (opposite spins) from Fermi-correlation effects embodied by the equal-spin terms.

The study of the SP-TPS tensor for Heisenberg chains gave us the chance to investigate how different spin states affect the electron mobility. It has to be noted that we demonstrated a rule of thumb which connects the closure of the energy gap with divergence of the SP-TPS tensor. Moreover, an analytical expression was derived for the SP-TPS tensor of a Heisenberg chain as a function of system size and the z-projected spin quantum number s_z.

A quantitative description of quantum entanglement can be achieved by means of an other machinery, that is, quantum information theory (QIT)[42, 92–101], which allows a direct analysis of the reduced density matrix. Although these tools are strongly dependent on the orbital basis employed, we discussed how they can be employed to gain information regarding the metallic/insulating character of the wave function in one-dimensional quantum-chemical systems (see **Paper M2**). In order to investigate intrinsic changes in the wave function in different regimes, we first studied the orbital entanglement, which can be measured by the mutual information. A deeper insight into the processes responsible for entanglement was achieved by the analysis of the elements of the two-orbital reduced density matrix, which describe the different transition probabilities. In a localized-orbital basis, these could be understood as spin-flipping and hopping terms. The latter are connected to the electric conductivity. We also analyzed the block von Neumann entropy of a segment of finite chains. Indeed,

for gapless systems this diverges logarithmically with block size, while converges for gapped systems. Therefore we could investigate this behavior and use it as an index of MITs. Lithium rings with s-like localized basis only were investigated as a quantum-chemical analogous of the Hubbard chain, which is the minimal model to describe MITs. Also more complex systems, beryllium rings, were studied for different internuclear distance regimes, where they present different metallic/insulating behaviors. Particular focus was also given on the role played by the orbital basis on the performance of the *ab-initio* density matrix renormalization group (DMRG)[82–91]. By using both canonical orbitals and localized orbitals for the description of beryllium rings, we realized that using the latter requires less computational effort to achieve the same accuracy. This is because of the lower entanglement between localized orbitals with respect to canonical orbitals. Understanding the dependence of entanglement on the orbital basis is fundamental for improving the performance of tensor-product based methods such as DMRG. Indeed, the results of these investigations on beryllium rings were exploited in recent works[194] to develop an automatized algorithm which optimizes the orbital basis for reducing entanglement and speeding up the DMRG procedure. Future investigations are being carried out in this direction.

Accurate DMRG results were used as benchmark for another quantum-chemical method, the method of increments (MoI)[64–76] . The power of this approach lies in its reduced scaling, which allows very accurate electron-correlation calculations of extended and periodic systems. The description of strongly correlated systems with pronounced multireference character is, however, problematic via the standard formalism of the MoI. Therefore, in this work we presented some novel variants of the method of increments using beryllium rings, as test studies which required an accurate description of both static and dynamical correlation (see **Papers M3** and **M4**). First, we discussed the complete active space (CAS)-MoI formalism which yields most of the correlation energy that can be obtained at the CAS-SCF level. On top of such calculations, any nearly size-extensive multireference (MR) method can be applied in order to calculate the remaining dynamical correlation energy. The applicability of this MR-MoI was shown to be strongly dependent on the method applied for large systems, since if size-extensivity is not correctly described, large errors are introduced in the individual increments. After discussing the accuracy of these methods for the Be_6 ring, we applied them to much larger rings, for which standard methods are not applicable. This allowed the extrapolation of the correlation energy for an infinite chain.

Through these strategies we achieved very accurate correlation energies, but we could not describe the whole dissociation curve in a size-consistent manner. To overcome this problem, we introduced a more sophisticated approach, the two-state constant-coupling (TSCC)-MoI (see **Paper M5**). This novel method allows accurate calculations (in comparison to DMRG) of ground-state dissociation curves for extended systems. Moreover, the TSCC-MoI gives access, in principle, to excited states, which is an appealing perspective, although for the moment the results are not as accurate as they are for the

ground state. The analysis of the correlated DMRG wave function revealed that this discrepancy is mainly due to a poor choice of the reference for the excited state. Work is in progress in the workgroup Paulus to improve the accuracy of the TSCC-MoI for excited states and to extend the procedure to a larger number of states. This is a fascinating prospective since the TSCC-MoI would allow the investigation of a part of the excitation spectrum via a low scaling local approach. Another interesting perspective for the development of the method of increments is given by its possible combination with DMRG, which could be applied to estimate the most suitable orbital basis for the MoI many-body expansion.

Finally, exploiting the power of the MoI formalism to calculate properties for extended systems, we proposed a strategy to calculate the SS-TPS tensor via the MoI. Indeed, the calculation of the TPS tensor requires an accurate description of electron correlation for extended systems in order to yield important information regarding the electron conductivity. The MoI allows that. The preliminary results which were presented here show how such a strategy yields good results for the Be_6 rings. This is an appealing direction which will be investigated further in the future.

In conclusion, one of the main points of this thesis concerned the analysis of the effects of electron correlation in the framework of metal-insulator transitions. This was done by studying the TPS tensor, which yields an indirect evaluation of entanglement by measuring the electron mobility, and by directly analyzing the reduced density matrix through quantum information theory. A consistent part of this work dealt with the development of new approaches. Firstly, we introduced and tested the novel SP-TPS tensor, which investigates spin mobility and spin entanglement. Its application to different spin states of Heisenberg chains allowed us to derive some interesting relations for the TPS tensor. Secondly, the MoI was extensively applied and new formalisms to treat strongly correlated systems were developed. In particular the novel TSCC-MoI solved the lack of size-consistency of the standard MoI and allowed the description of whole dissociation curves. Finally, a new scheme for the calculation of the TPS tensor via the MoI was presented and succesfully tested.

References

[1] C. Cen, S. Thiel, G. Hammerl, C. W. Schneider, K. E. Andersen, C. S. Hellberg, J. Mannhart, and J. Levy, Nature Materials **7**, 298 (2008).

[2] T. Chen, K. V. Reich, N. J. Kramer, H. Fu, U. R. Kortshagen, and B. I. Shklovskii, Nature Materials **15**, 299 (2015).

[3] K. Held, G. Keller, V. Eyert, D. Vollhardt, and V. I. Anisimov, Physical Review Letters **86**, 5345 (2001).

[4] R. Palai, R. S. Katiyar, H. Schmid, P. Tissot, S. J. Clark, J. Robertson, S. A. T. Redfern, G. Catalan, and J. F. Scott, Physical Review B **77**, 014110 (2008).

[5] L. A. Ponomarenko, A. K. Geim, A. A. Zhukov, R. Jalil, S. V. Morozov, K. S. Novoselov, I. V. Grigorieva, E. H. Hill, V. V. Cheianov, V. I. Fal'ko, K. Watanabe, T. Taniguchi, and R. V. Gorbachev, Nature Physics **7**, 958 (2011).

[6] B. Radisavljevic and A. Kis, Nature Materials **12**, 815 (2013).

[7] V. Kerala Varma and S. Pilati, Physical Review B **92**, 134207 (2015).

[8] M. Gatti, G. Panaccione, and L. Reining, Physical Review Letters **114**, 116402 (2015).

[9] N. Mott, *Metal-Insulator Transitions*, Taylor & Francis, 1990.

[10] F. Gebhard, *The Mott Metal-Insulator Transition: Models and Methods*, Springer Verlag, Berlin, Heidelberg, 1997.

[11] M. Imada, A. Fujimori, and Y. Tokura, Reviews of Modern Physics **70**, 1039 (1998).

[12] R. Dreizler and E. Gross, *Density Functional Theory*, Springer Verlag, Berlin, 1990.

[13] H. Eschrig, *The Fundamentals of Density Functional Theory*, B. C. Teubner Verlag, Stuttgart, 1996.

[14] W. Kohn and L. J. Sham, Physical Review **140**, A1133 (1965).

[15] C. J. Cramer and D. G. Truhlar, Physical Chemistry Chemical Physics **11**, 10757 (2009).

[16] A. J. Cohen, P. Mori-Sánchez, and W. Yang, Chemical Reviews **112**, 289 (2012).

[17] H. Bethe, Annalen der Physik **392**, 55 (1928).

[18] A. Sommerfeld, Zeitschrift für Physik **47**, 1 (1928).

[19] F. Bloch, Zeitschrift für Physik **57**, 545 (1929).

[20] A. H. Wilson, Proceedings of the Royal Society of London A **133**, 458 (1931).

[21] A. H. Wilson, Proceedings of the Royal Society of London A **134**, 277 (1931).

[22] R. H. Fowler, Proceedings of the Royal Society of London A **140**, 505 (1933).

[23] R. H. Fowler, Proceedings of the Royal Society of London A **141**, 56 (1933).

[24] N. Ashcroft and N. Mermin, *Solid State Physics*, HRW international editions, Holt, Rinehart and Winston, 1976.

[25] R. Peierls, *Quantum Theory of Solids*, International Series of Monographs on Physics, Clarendon Press, 1996.

[26] P. W. Anderson, Physical Review **109**, 1492 (1958).

[27] P. W. Anderson, Reviews of Modern Physics **50**, 191 (1978).

[28] J. H. de Boer and E. J. W. Verwey, Proceedings of the Physical Society **49**, 59 (1937).

[29] N. F. Mott and R. Peierls, Proceedings of the Physical Society **49**, 72 (1937).

[30] N. F. Mott, Proceedings of the Physical Society A **62**, 416 (1949).

[31] N. F. Mott, Canadian Journal of Physics **34**, 1356 (1956).

[32] N. F. Mott, Philosophical Magazine **6**, 287 (1961).

[33] N. F. Mott, Reviews of Modern Physics **40**, 677 (1968).

[34] J. Hubbard, Proceedings of the Royal Society of London A **276**, 238 (1963).

[35] J. Hubbard, Proceedings of the Royal Society of London A **277**, 237 (1964).

[36] J. Hubbard, Proceedings of the Royal Society of London A **281**, 401 (1964).

[37] W. Kohn, Physical Review **133**, A171 (1964).

[38] R. Nandkishore and D. A. Huse, Annual Review of Condensed Matter Physics **6**, 15 (2015).

[39] D. M. Basko, I. L. Aleiner, and B. L. Altshuler, On the problem of many-body localization, in *Problems of Condensed Matter Physics*, Oxford University Press, 2007.

[40] D. Basko, I. Aleiner, and B. Altshuler, Annals of Physics **321**, 1126 (2006).

[41] B. Bauer and C. Nayak, Journal of Statistical Mechanics: Theory and Experiment **2013**, P09005 (2013).

[42] J. Eisert, M. Cramer, and M. B. Plenio, Reviews of Modern Physics **82**, 277 (2010).

[43] M. Friesdorf, A. H. Werner, W. Brown, V. B. Scholz, and J. Eisert, Physical Review Letters **114**, 1 (2015).

[44] R. Resta and S. Sorella, Physical Review Letters **82**, 370 (1999).

[45] R. Resta, Physical Review Letters **95**, 196805 (2005).

[46] I. Souza, T. Wilkens, and R. M. Martin, Physical Review B **62**, 25 (1999).

[47] R. Resta, Physical Review Letters **96**, 137601 (2006).

[48] R. Resta, The Journal of Chemical Physics **124**, 104104 (2006).

[49] O. Brea, M. E. Khatib, C. Angeli, G. L. Bendazzoli, S. Evangelisti, and T. Leininger, Journal of Chemical Theory and Computation **9**, 5286 (2013).

[50] M. El Khatib, T. Leininger, G. L. Bendazzoli, and S. Evangelisti, Chemical Physics Letters **591**, 58 (2014).

[51] P. Pulay, Chemical Physics Letters **100**, 151 (1983).

[52] P. Pulay and S. Saebø, Theoretica Chimica Acta **69**, 357 (1986).

[53] G. Stollhoff and A. Heilingbrunner, Zeitschrift für Physik B **83**, 85 (1991).

[54] R. Pardon, J. Gräfenstein, and G. Stollhoff, Physical Review B **51**, 10556 (1995).

[55] K. Kitaura, E. Ikeo, T. Asada, T. Nakano, and M. Uebayasi, Chemical Physics Letters **313**, 701 (1999).

[56] M. Schütz, The Journal of Chemical Physics **113**, 9986 (2000).

[57] M. Schütz and H. J. Werner, The Journal of Chemical Physics **114**, 661 (2001).

[58] M. Schütz, Physical Chemistry Chemical Physics **4**, 3941 (2002).

[59] M. Schütz, The Journal of Chemical Physics **116**, 8772 (2002).

[60] M. Schütz, O. Masur, and D. Usvyat, The Journal of Chemical Physics **140**, 244107 (2014).

[61] M. Schwilk, D. Usvyat, and H. J. Werner, The Journal of Chemical Physics **142**, 121102 (2015).

[62] C. Pisani, L. Maschio, S. Casassa, M. Halo, M. Schütz, and D. Usvyat, Journal of Computational Chemistry **29**, 2113 (2008).

[63] C. Pisani, M. Schütz, S. Casassa, D. Usvyat, L. Maschio, M. Lorenz, and A. Erba, Physical Chemistry Chemical Physics **14**, 7615 (2012).

[64] H. Stoll, Chemical Physics Letters **191**, 548 (1992).

[65] H. Stoll, Physical Review B **46**, 6700 (1992).

[66] H. Stoll, B. Paulus, and P. Fulde, Chemical Physics Letters **469**, 90 (2009).

[67] H. Stoll, Molecular Physics **108**, 243 (2010).

[68] B. Paulus, Chemical Physics Letters **371**, 7 (2003).

[69] B. Paulus, Physics Reports **428**, 1 (2006).

[70] E. Voloshina and B. Paulus, Physical Review B **75**, 245117 (2007).

[71] I. Schmitt, K. Fink, and V. Staemmler, Physical Chemistry Chemical Physics **11**, 11196 (2009).

[72] C. Müller, D. Usvyat, and H. Stoll, Physical Review B **83**, 245136 (2011).

[73] V. Staemmler, Journal of Physical Chemistry A **115**, 7153 (2011).

[74] J. Friedrich, M. Hanrath, and M. Dolg, The Journal of Chemical Physics **126**, 154110 (2007).

[75] J. Friedrich and M. Dolg, The Journal of Chemical Physics **129**, 244105 (2008).

[76] J. Friedrich, Journal of Chemical Theory and Computation **8**, 1597 (2012).

[77] C. Müller, B. Paulus, and K. Hermansson, Surface Science **603**, 2619 (2009).

[78] L. Hammerschmidt, C. Müller, and B. Paulus, The Journal of Chemical Physics **136**, 124117 (2012).

[79] L. Hammerschmidt, L. Maschio, C. Müller, and B. Paulus, Journal of Chemical Theory and Computation **11**, 252 (2015).

[80] J. Yang and M. Dolg, The Journal of Chemical Physics **127**, 084108 (2007).

[81] J. Friedrich, S. Coriani, T. Helgaker, and M. Dolg, The Journal of Chemical Physics **131**, 154102 (2009).

[82] S. R. White, Physical Review Letters **69**, 2863 (1992).

[83] S. R. White, Physical Review B **48**, 10345 (1993).

[84] Ö. Legeza, R. Noack, J. Sólyom, and L. Tincani, Applications of quantum information in the density-matrix renormalization group, in *Computational Many-Particle Physics*, edited by H. Fehske, R. Schneider, and A. Weiße, Berlin, Heidelberg, 2008, Springer Verlag.

[85] G. K.-L. Chan and D. Zgid, Annual Reports in Computational Chemistry **5**, 149 (2009).

[86] K. H. Marti and M. Reiher, Zeitschrift für Physikalische Chemie **224**, 583 (2010).

[87] U. Schollwöck, Annals of Physics **326**, 96 (2011).

[88] R. Olivares-Amaya, W. Hu, N. Nakatani, S. Sharma, J. Yang, and G. K.-L. Chan, The Journal of Chemical Physics **142**, 034102 (2015).

[89] V. Murg, F. Verstraete, R. Schneider, P. R. Nagy, and Ö. Legeza, Journal of Chemical Theory and Computation **11**, 1027 (2015).

[90] S. Wouters and D. Van Neck, The European Physical Journal D **68**, 272 (2014).

[91] S. Szalay, M. Pfeffer, V. Murg, G. Barcza, F. Verstraete, R. Schneider, and Ö. Legeza, International Journal of Quantum Chemistry **115**, 1342 (2015).

[92] Ö. Legeza and J. Sólyom, Physical Review B **68**, 195116 (2003).

[93] J. Rissler, R. M. Noack, and S. R. White, Chemical Physics **323**, 519 (2006).

[94] G. Barcza, Ö. Legeza, K. H. Marti, and M. Reiher, Physical Review A **83**, 12508 (2011).

[95] G. Vidal, J. I. Latorre, E. Rico, and A. Kitaev, Physical Review Letters **90**, 227902 (2003).

[96] Ö. Legeza and J. Sólyom, Physical Review B **70**, 205118 (2004).

[97] J. Eisert and H. J. Briegel, Physical Review A **64**, 022306 (2001).

[98] M. B. Plenio, J. Eisert, J. Dreißig, and M. Cramer, Physical Review Letters **94**, 060503 (2005).

[99] J. Eisert and M. B. Plenio, International Journal of Quantum Information **1**, 479 (2003).

[100] J. Eisert and D. Gross, Multi-particle entanglement, in *Quantum Information Theory*, edited by D. Bruss and L. G, Wenheim, 2007, VCH.

[101] K. Kieling and J. Eisert, Percolation in quantum computation and communication, in *Quantum Percolation and Breakdown*, edited by K. B. Chakrabarti, K. K. Bardhan, and K. A. Sen, Berlin, Heidelberg, 2009, Springer Verlag.

[102] I. V. Oseledets, SIAM Journal on Scientific Computing **33**, 2295 (2011).

[103] R. Hübener, A. Mari, and J. Eisert, Physical Review Letters **110**, 040401 (2013).

[104] J. Eisert, Modeling and Simulation **3**, 39 (2013).

[105] M. Kliesch, D. Gross, and J. Eisert, Physical Review Letters **113**, 160503 (2014).

[106] M. Fannes, B. Nachtergaele, and R. F. Werner, Communications in Mathematical Physics **144**, 443 (1992).

[107] E. Schrödinger, Annalen der Physik **384**, 361 (1926).

[108] M. Born and R. Oppenheimer, Annalen der Physik **20**, 457 (1927).

[109] P. A. M. Dirac, *The Principles of Quantum Mechanics*, Clarendon, Oxford, 1930.

[110] D. Andrae, Total state designation for electronic states of periodic systems, in *Proceedings of the 38th Annual Condensed Matter and Materials Meeting - Waiheke Island, Auckland, NZ*, edited by T. Söhnel, 2014.

[111] J. C. Slater, Phys. Rev. **34**, 1293 (1929).

[112] W. Heisenberg, Zeitschrift für Physik **38**, 411 (1926).

[113] P. A. M. Dirac, Proceedings of the Royal Society of London A **112**, 661 (1926).

[114] D. R. Hartree, Mathematical Proceedings of the Cambridge Philosophical Society **24**, 89 (1928).

[115] V. Fock, Zeitschrift für Physik **61**, 126 (1930).

[116] J. A. Pople and R. K. Nesbet, The Journal of Chemical Physics **22**, 571 (1954).

[117] C. C. J. Roothaan, Reviews of Modern Physics **23**, 69 (1951).

[118] G. G. Hall, Proceedings of the Royal Society of London A **205**, 541 (1951).

[119] T. Koopmans, Physica **1**, 104 (1934).

[120] E. U. Condon, Physical Review **36**, 1121 (1930).

[121] L. Brilluoin, Helvetica Physica Acta **7**, 33 (1934), Supp. II.

[122] R. J. Bartlett, Annual Review of Physical Chemistry **32**, 359 (1981).

[123] P. R. Taylor, *Coupled-cluster Methods in Quantum Chemistry*, Springer Verlag, Berlin, Heidelberg, 1994.

[124] S. R. Langhoff and E. R. Davidson, International Journal of Quantum Chemistry **8**, 61 (1974).

[125] L. Meissner, Chemical Physics Letters **146**, 204 (1988).

[126] J. Čížek, The Journal of Chemical Physics **45**, 4256 (1966).

[127] J. Cizek and J. Paldus, Physica Scripta **21**, 251 (1980).

[128] R. J. Bartlett, The Journal of Physical Chemistry **93**, 1697 (1989).

[129] J. Gauss, *Coupled-cluster Theory*, John Wiley Sons, Ltd, 2002.

[130] R. J. Bartlett and M. Musiał, Reviews of Modern Physics **79**, 291 (2007).

[131] J. Čížek, *On the Use of the Cluster Expansion and the Technique of Diagrams in Calculations of Correlation Effects in Atoms and Molecules*, John Wiley Sons, Inc., 2007.

[132] T. D. Crawford and H. F. Schaefer, *An Introduction to Coupled Cluster Theory for Computational Chemists*, John Wiley Sons, Inc., 2007.

[133] K. Raghavachari, G. W. Trucks, J. A. Pople, and M. Head-Gordon, Chemical Physics Letters **157**, 479 (1989).

[134] R. J. Bartlett, J. Watts, S. Kucharski, and J. Noga, Chemical Physics Letters **165**, 513 (1990).

[135] J. F. Stanton, Chemical Physics Letters **281**, 130 (1997).

[136] T. J. Lee and P. R. Taylor, International Journal of Quantum Chemistry **36**, 199 (1989).

[137] B. O. Roos, International Journal of Quantum Chemistry **18**, 175 (1980).

[138] B. O. Roos, P. R. Taylor, and P. E. Sigbahn, Chemical Physics **48**, 157 (1980).

[139] P. E. M. Siegbahn, J. Almlöf, A. Heiberg, and B. O. Roos, The Journal of Chemical Physics **74**, 2384 (1981).

[140] R. J. Buenker and S. D. Peyerimhoff, Theoretica Chimica Acta **35**, 33 (1974).

[141] H. Werner and E. Reinsch, The Journal of Chemical Physics **76**, 3144 (1982).

[142] R. J. Gdanitz and R. Ahlrichs, Chemical Physics Letters **143**, 413 (1988).

[143] U. S. Mahapatra, B. Datta, and D. Mukherjee, The Journal of Chemical Physics **110**, 6171 (1999).

[144] F. A. Evangelista, W. D. Allen, and H. F. Schaefer, The Journal of Chemical Physics **127**, 024102 (2007).

[145] F. A. Evangelista, E. Prochnow, J. Gauss, and H. F. Schaefer, The Journal of Chemical Physics **132**, 074107 (2010).

[146] C. Møller and M. S. Plesset, Physical Review **46**, 618 (1934).

[147] J. Boström, F. Aquilante, T. B. Pedersen, and R. Lindh, Journal of Chemical Theory and Computation **5**, 1545 (2009).

[148] R. Łazarski, A. M. Burow, and M. Sierka, Journal of Chemical Theory and Computation **11**, 3029 (2015).

[149] J. A. Pople, R. Krishnan, H. B. Schlegel, and J. S. Binkley, International Journal of Quantum Chemistry **14**, 545 (1978).

[150] J. Pipek and P. G. Mezey, The Journal of Chemical Physics **90**, 4916 (1989).

[151] J. M. Foster and S. F. Boys, Reviews of Modern Physics **32**, 300 (1960).

[152] S. F. Boys, Rev. Mod. Phys. **32**, 296 (1960).

[153] G. Stollhoff and P. Fulde, Zeitschrift für Physik B **26**, 257 (1977).

[154] G. Stollhoff, The Journal of Chemical Physics **105**, 227 (1996).

[155] C. Pisani, M. Busso, G. Capecchi, S. Casassa, R. Dovesi, L. Maschio, C. Zicovich-Wilson, and M. Schütz, Journal of Chemical Physics **122**, 094113 (2005).

[156] S. Sæbø and P. Pulay, The Journal of Chemical Physics **86**, 914 (1987).

[157] H. J. Werner et al., Molpro, version 2015.1, a package of ab initio programs, 2015, see http://www.molpro.net.

[158] H.-J. Werner, P. J. Knowles, G. Knizia, F. R. Manby, and M. Schütz, Wiley Interdisciplinary Reviews: Computational Molecular Science **2**, 242 (2012).

[159] E. Voloshina and B. Paulus, Journal of Chemical Theory and Computation **10**, 1698 (2014).

[160] K. G. Wilson, Reviews of Modern Physics **47**, 773 (1975).

[161] O. Legeza and J. Sólyom, Phys. Rev. Lett. **96**, 116401 (2006).

[162] K. Boguslawski, P. Tecmer, Örs Legeza, and M. Reiher, The Journal of Physical Chemistry Letters **3**, 3129 (2012).

[163] J. Von Neumann, *Mathematische Grundlagen der Quantenmechanik*, Springer Verlag, Berlin, 1932.

[164] J. E. Atkins, E. G. Boman, and B. Hendrickson, SIAM Journal on Computing **28**, 297 (1998).

[165] M. Fiedler, Czechoslovak Mathematical Journal **23**, 298 (1973).

[166] M. Fiedler, Czechoslovak Mathematical Journal **25**, 619 (1975).

[167] Ö. Legeza, J. Röder, and B. A. Hess, Physical Review B **67**, 125114 (2003).

[168] G. Barcza, R. M. Noack, J. Sólyom, and O. Legeza, Physical Review B **92**, 125140 (2015).

[169] P. Calabrese and J. Cardy, **06002**, 33 (2004).

[170] K. Aidas et al., WIREs Computational Molecular Science **4**, 269 (2014).

[171] Dalton: A molecular electronic structure program, 2005, see http://www.kjemi.uio.no.

[172] G. L. Bendazzoli, M. El Khatib, S. Evangelisti, and T. Leininger, Journal of Computational Chemistry **35**, 802 (2014).

[173] M. El Khatib, G. L. Bendazzoli, S. Evangelisti, W. Helal, T. Leininger, L. Tenti, and C. Angeli, The Journal of Physical Chemistry A **118**, 6664 (2014).

[174] G. L. Bendazzoli, S. Evangelisti, A. Monari, B. Paulus, and V. Vetere, Journal of Physics: Conference Series **117**, 012005 (2008).

[175] V. Vetere, A. Monari, G. L. Bendazzoli, S. Evangelisti, and B. Paulus, The Journal of Chemical Physics **128**, 024701 (2008).

[176] G. L. Bendazzoli, S. Evangelisti, A. Monari, and R. Resta, The Journal of Chemical Physics **133**, 064703 (2010).

[177] E. Giner, G. L. Bendazzoli, S. Evangelisti, and A. Monari, The Journal of Chemical Physics **138**, 074315 (2013).

[178] Ö. Legeza, QCDMRG-Budapest a program package to carry out quantum chemical DMRG calculations, HAS-RISPO, 2000-2015.

[179] G. L. Bendazzoli and S. Evangelisti, The Journal of Chemical Physics **98**, 3141 (1993).

[180] G. L. Bendazzoli and S. Evangelisti, International Journal of Quantum Chemistry **48**, 287 (1993).

[181] L. Gagliardi, G. L. Bendazzoli, and S. Evangelisti, Journal of Computational Chemistry **18**, 1329 (1997).

[182] M. E. Khatib and E. Fertitta, Heisenberg: Code under mit license, 2014.

[183] M. G. Zacher, A. Dorneich, C. Gröber, R. Eder, and W. Hanke, The metal-insulator transition in the hubbard model, in *High Performance Computing in Science and Engineering '99: Transactions of the High Performance Computing Center Stuttgart (HLRS) 1999*, edited by E. Krause and W. Jäger, Berlin, Heidelberg, 2000, Springer Verlag.

[184] A. Balachandran, *Hubbard Model and Anyon Superconductivity*, Lecture notes in physics, World Scientific, 1990.

[185] A. Auerbach, *Interacting Electrons and Quantum Magnetism*, Graduate Texts in Contemporary Physics, Springer New York, 1998.

[186] H. Bethe, Zeitschrift für Physik **71**, 205 (1931).

[187] C. L. Cleveland and R. Medina A., American Journal of Physics **44**, 44 (1976).

[188] M. C. Heaven, J. M. Merritt, and V. E. Bondybey, Annual Review of Physical Chemistry **62**, 375 (2011).

[189] W. Helal, S. Evangelisti, T. Leininger, and A. Monari, Chemical Physics Letters **568**, 49 (2013).

[190] J. M. Merritt, V. E. Bondybey, and M. C. Heaven, Science **324**, 1548 (2009).

[191] K. Patkowski, R. Podeszwa, and K. Szalewicz, Journal of Physical Chemistry A **111**, 12822 (2007).

[192] J. Koput, Physical Chemistry Chemical Physics **13**, 20311 (2011).

[193] X. W. Sheng, X. Y. Kuang, P. Li, and K. T. Tang, Physical Review A **88**, 1 (2013).

[194] C. Krumnow, Ö. Legeza, and J. Eisert, (2015), arXiv:1504.00042 [quant-ph].